Improving Control Mechanism of an Active Air-Suspension System

Alireza Kazemeini

Submitted to the
Institute of Graduate Studies and Research
in partial fulfilment of the requirements for the Degree of

Master of Science
in
Mechanical Engineering

Eastern Mediterranean University
January 2013
Gazimağusa, North Cyprus

Approval of the Institute of Graduate Studies and Research

Prof. Dr. Elvan Yılmaz
Director

I certify that this thesis satisfies the requirements as a thesis for the degree of Master of Science in Mechanical Engineering.

Assoc. Prof. Dr. Uğur Atikol
Chair, Department of Mechanical Engineering

I certify that I have read this thesis and that in our opinion it is fully adequate in scope and quality as a thesis for the degree of Master of Science in Mechanical Engineering.

Asst. Prof. Dr. Hasan Hacışevki
Supervisor

Examining Committee

1. Prof. Dr. Majid Hashemipour
2. Asst. Prof. Dr. Hasan Hacışevki
3. Asst. Prof. Dr. Nariman Özada

ABSTRACT

The technology of pneumatic vibration isolation for air-suspensions is developing gradually. As environmental vibroisolation requirements on precision equipment and air-suspensions become more stringent, the use of pneumatic isolators has become more popular, and their performance is subsequently required to be further improved. Due to air-suspension systems prevalence in heavy vehicles todays, improving control strategy and software base reformation can be an economical solution for performance improvement.

In this study an active control technique, based on pressure is applied to a pneumatic isolator to enhance the isolation performance in the low frequency range where the passive techniques have difficulties. An air spring from air suspension system was modelled as the pneumatic isolator in a quarter-car model. The test plan for suspension model was in two approaches, model based simulation and experimental test, in order to evaluate the quarter-car suspension system. First, a mathematical model of an air-suspension for a quarter-car was built, in MATLAB-Simulink program. Then, the suspension prototype was prepared for the approach of experimental study. The experimental test design was based on physical equipment's and performed in lab-view. Body acceleration, tire forces and suspension travel were outputs of experimental test. The optimization was investigated in two parts of dynamic performance including handling and comfort, and suspension travel as a structural performance. The results from experimental study were compared with

simulative test from Simulink software in order to evaluate the percentage of simulation accuracy of active and passive approaches.

The result comparison between active and passive suspension demonstrates 11.51% acceleration reduction during experimental test. Additionally, amplitude of suspension travel was reduced until 11.94% which shows structural improvement in vehicles suspension. Also dynamic forces were applied to the wheel, didn’t increase but also reduced until 3.04%. As conclusion, the new suspension performance was increased by applying control on system.

Keywords: suspension, pneumatic, air-spring, control strategy, simulation and experimental tests.

ÖZ

Havalı süspansiyon sistemleri'nin kullanımı araçların sürüş konforunu, dinamik davranışını ve yükseklik ayarlarını geliştirdiği için havalı titreşim söndürücülerin kontrol sistemleri modern koltuk, kabin ve şasi uygulamalarında gittikçe önem kazanmaktadır. Havalı süspansiyon sistemlerinin hava titreşim söndürücüsü teknolojisi günden güne gelişmekedir. Hassas cihazlara çevreden gelen titreşimin etkileri ve havalı titreşim söndürücülerin üzerlerindeki performans etkilerinin daha araştırılması gerekir. Havalı söndürücülerin dinamik performansları limitlidir ve alçak frekanslarda tasarım parametreleri daha karmaşık hale gelmektedir, bu etki rezonans frekansı veya hava bölmesinin hacmi tarafından sınırlanmaktadır. Aktif süspansiyon sistemi gelişen performans yaklaşımları için düşünülmüştür. Bugün havalı süspansiyon sistemleri birçok araçta yaygın olarak kullanılmaktadır, kontrol stratejisinin geliştirilmesi ve yazılım uygulamaları ile performans gelişimine ekonomik çözüm getirmek amaçlanmaktadır.

Bu çalışmada basınca bağlı aktif kontrol tekniği pasif tekniğin zorlandığı alçak frekanstaki izolasyon performansını artırmak için pnömatik izolatöre uygulanmıştır. Havalı süspansiyon sistemindeki bir hava yayı çeyrek araç modeli pnömatik izolatörü olarak modellenmiştir. Çeyrek araç süspansiyon sistemini değerlendirmek amacıyla süspansiyon modeli için test planı, simülasyon ve deneysel test olarak iki kısımda ele alınmıştır. Öncelikle pasif, aktif ve pnömatik aktif süspansiyon sistemi için MATLAB-Simulink programında bir bilgisayar modeli inşa edilmiştir. Sonra, deneysel çalışma yaklaşımı için süspansiyon prototip hazırlanmıştır. Bu çalışma için

inşa edilen deneysel model, yükseklik sensörleri, basınç sensörü, pnömatik aktüatörler ve denetleyici ihtiva eden çeyrek araç modeli oldu. Deneysel test çıkışı ivme ve mesafe olmuştur. Gövde ve tekerleğin ivmesi ile aralarındaki mesafe süspansiyon performans değerlendirmesinde önemli bir rol oynar. Optimizasyon dinamik performansın iki öğesi olan yol tutuşu ve konfor için incelenmiş ve yapısal performans olarak süspansiyon hareketi araştırılmıştır. Deneysel çalışmanın sonuçları aktif ve pasif yaklaşımların simülasyon doğruluk yüzdesini değerlendirmek için Simulink yazılımı sonuçları ile karşılaştırıldı.

Aktif ve pasif arasındaki sonuçların karşılaştırılması sonucunda deneysel model gövdesinde %11.51 ivme azalması görülmüştür. Ayrıca, süspansiyon hareketi genliği % 11.94 kadar düşmüş ve araç süspansiyonunda yapısal iyileşme göstermiştir. Tekerleklere uygulanan dinamik kuvvetler artmamış fakat % 3,04 kadar azalmıştır. Sonuç olarak, sistem üzerinde kontrol uygulanarak yeni süspansiyon performans artırılmıştır.

Anahtar kelimeler: süspensiyon, pnömatik, hava yayı, kontrol stratejisi, simülasyon ve deneysel test.

ACKNOWLEDGMENTS

It is a pleasure to express my gratitude to those who made this thesis possible such as my supervisor Asst. Prof. Dr. Hasan Hacışevki for his excellent guidance, caring and patience and his encouragement, supervision and support from preliminary to the concluding level enabled me to do this research.

I would like to thank Prof. Dr. M.Hashemipour and Mr.zafer Mulla for their encouragement and support during my research on this project.

I would like to thank my friends Dr. Ehsan Kiani and Mr. Muhammad Abu Bekir and others who were always willing to help and encouraged me in this report.

At last, I would like to thank my parents who were always supporting me and encouraging me with their best wishes.

TABLE OF CONTENTS

LIST OF TABLES

LIST OF FIGURES

LIST OF ABBREVIATIONS

CES	Continuously Controlled Electronic Suspension
5/3	Five connections and three conditions
DAQ	Data acquisition card
TDC	Time delay control
RMS	Root-Mean-Square
MPTP	Maximum Peak To Peak
PSI	pound per square inch
DC	Direct current
V	Volt
Susp,	Suspension

LIST OF SYMBULS

r	Road disturbance
X_b	Body displacement
$\dot{X}_b$	Body velocity
$\ddot{X}_b$	Body acceleration
X_w	Wheel displacement
$\dot{X}_w$	Wheel velocity
$\ddot{X}_w$	Wheel Acceleration
X_r	Road displacement
$\dot{X}_r$	Road velocity
h_b	Stable position of body
h_w	Stable position of wheel
M_b	Body mass
M_w	Wheel mass
M_{total}	Total suspension mass
K	Spring stiffness (N/m)
K_t	Tire stiffness
C	viscous damping
C_t	Tire structural damp (Nm/s)
F	force (N)
u	Control input
g	Gravity (m/s^2)

P	pressure (N/m2)
A	area (m2)
R	the universal gas constant (=286.9 (J/(kg K)))
T	temperature (K)
V	volume (m3)
t	time (s)
Δ	difference
ρ	density (kg/m3)
d	diagonal
e	Error
Fr	Friction
F_t	Tire force
G	gravity
Ω	ohm

Chapter 1

INTRODUCTION

Many important automotive innovations are based on significant improvements of formerly pure mechanical subsystems, by using integrated electronics together with complex information processing [10]. Active suspension as a sample of mechatronic systems, tries to show the importance of using integrated electronics together with complex information processing and its results in mechanical system performance.

The purpose of this chapter is to provide an introduction showing the overview of this research, in four different parts. First it describes the motivation of the research. Then, the determined objectives of the research will be explained. The approach, which is based on the objectives and finally the classification of the manuscript, will be explained.

1.1 Motivation

Vibration isolation has become significant in many industries to protect instruments, driver seats, vehicle cabins and passenger cars, from vibration and its affects. For example, Precision instruments such as laser systems or electron-beam microscopes are highly sensitive to environmental vibrations. As more precision is needed, requirements on vibration isolation have become more essential [4].

In general, ride comfort, road handling, and stability are the most important factors in evaluating suspension performance. Ride comfort is proportional to the absolute acceleration of the vehicle body, while road handling is linked to the relative displacement between vehicle body and the tires. On the other hand, stability of vehicles is related to the tire-ground contact. The main concern in suspension design and control is the fact that currently, achieving improvement in these three objectives poses a challenge because these objectives will likely conflict with each other in the vehicle operating domain [6].

Ride comfort and road holding are in differential relation and they should be compromised with each other. Refer to structural limitations in passive suspension, a high performance ride comfort needs a soft spring and it also causes weak stability. [11]. Dampers Dry friction is another factor effecting ride comfort. If the road input cannot overcome on static friction, the system will be locked, which is called "boulevard jerk," [11].

1.2 Objectives

The objective of this research is to develop the control mechanism of an air-suspension by using Vibroisolation in air-spring with the aim of improving the dynamic behaviour of system. In order to achieve this goal, these specific objectives are determined:

• To study the background of active suspensions and their control strategies.

• To reveal proper active suspension and control strategy for air-suspension.

• To use air-spring as an active component and semi-active shock absorber co-operator, and applying a pneumatic Vibroisolation for passenger car approach.

• Improving air-suspension dynamic performance with control strategy and software base reformation.

• To find a simulation model for activation, such as mathematical equation or neural network to achieve better result conformity between simulation and experimental.

• To define a quarter-car suspension-test and relevant specifications.

• To build a mathematical and computer model of the overall system.

• To develop a prototype of the quarter-car suspension with the active air-spring, including development of the components of the active suspension.

• To design the simulation and experimental tests.

• To perform the simulation and experimental tests.

• To validate the simulation model by simulation and experimental results investigation.

• To evaluate the new suspension by comparing the passive results with active suspension results.

• To determine the conclusion of research based on the whole results.

1.3 Approach

The work presented in this thesis is active air-suspension system for a passenger car, to improve comfort, road handling and safety. The main control objectives of active vehicle suspension systems are to improve the ride comfort and handling performance of the vehicle by controlling actuator forces depending on feedback and feedforward information of the system obtained from sensors [12].

The general approach in this study is shown in fig.1.1, and the idea of applying force by pressure variation in air-spring was considered. In order to examine the new performance of system, many simulation model was prepared in MATLAB-

Simulink. Finally a simulation model in lab-view prepared and its experimental was considered to certify the result of simulation.

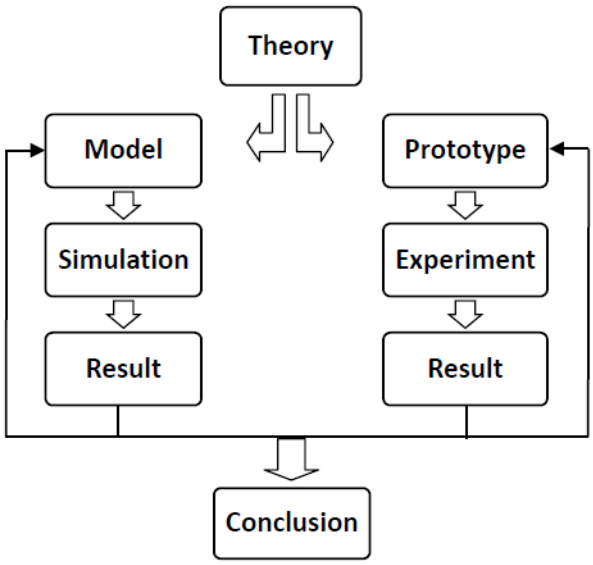

Figure 1.1: A schematic of research approach [5]

1.4 Outline

In order to achieve the objectives of this investigation, five steps were performed. In harmony with these steps, this thesis is organized in six succeeding chapters and finally conclusion and further study. These steps are presented here in this section.

The first step of the study was the background and literature review of the investigation. This was made in the subjects of the active suspension system of vehicles, pneumatic vibration isolation and their control strategies. These subjects are presented in the chapter 2 of this thesis. First, different kinds of active suspensions and some related control-strategies are explained. Then, the actuator system of active suspensions and pneumatic vibration isolation are described.

The Chapter 3 was designing and modelling of a new suspension system. The modelling included the mathematical modelling, derived from a physical model and finally a computer model using MATLAB-Simulink program. At first, the computer model was prepared in MATLAB-Simulink and then rewritten in lab-view, including the model of the actuator. Next, the model of the control system is presented. At the end of this step, the overall model involving all sub-models is completed.

Chapter 4 was the development of the prototype of the suspension system. The prototype was used for the experimental study of this research. At first, the control system, including hardware and software components is explained. The controller was a personal computer with proper software. This computer was connected to the system's inputs (i.e. sensors) and outputs (i.e. actuators) by using an interface card. After the control system, the building the pneumatic actuator system and relevant installation on the air-spring of the suspension system is presented.

Chapter 5 was the test design. The test design was similar for the simulation and experimental tests. For the experimental tests, an electric motor was running a conveyer and a road with some bumps and speed humps were simulated on it. In addition, a data acquisition system was attached with three position sensors in the experimental model. One of them was sensing road input to the system and the other two were sensing wheel and body displacement as output data. In this chapter, the test input and output as well as the analysis methods of the output data are determined.

Chapter 6 was the study of the results of the simulation and experimental tests. With a simple comparison between these two models, the validation of the simulation was performed. After that, performance of the active suspension was investigated by comparing the passive and active results. Two series of the results related to the vehicle body acceleration and the tire dynamic force were used to illustrate the stability and comfort respectively. At the end, all results were used in order to determine the conclusion of this study and provide some recommendations for future works. Finally, in chapter 7 the results of this study are concluded. The highlights, significant results, and the summary of the main works are presented. At the end, recommendations for future work are given.

Chapter 2

BACKGROUND AND LITERATURE REWIEW

2.1 Vehicle Suspension

One of challenges in every vehicle is performing comfort and handling at the same time. In some vehicles such as a city bus the importance of comfort is more. The merit of comfort is for passenger's welfare which is only achievable by decreasing stability and that's why mostly a city bus does not drive fast.

In contrast of this example, some vehicles such as speed race cars are using a suspension with high handling performance to increase the vehicle stability.

2.1.1 Ride Comfort

Ride comfort is term as one of suspension characteristics. It task is to provide passenger comfort in the vehicle or in other words, it is inversely proportional with body acceleration. Acceleration is the sensible factor by passenger and reducing acceleration result, is feeling more comfort for passengers.

2.1.2 Vehicle Handling

Vehicle handling is another suspension term to increase vehicle stability or road handling the effective character to improve vehicle handling is damping number. In a passive suspension, high handling will come off with increasing damping number.

2.1.3 Passive Suspension Compromise

In passive suspension, characters of comfort and handling are in a differential relation. That means a suspension with a week damper has high comfort performance and low body acceleration. In other hand, a suspension with a high damping has high stability and handling. However, it doesn't allow a free rapid motion in the wheel and this cause more acceleration in the body part, which reduces the term of ride comfort.

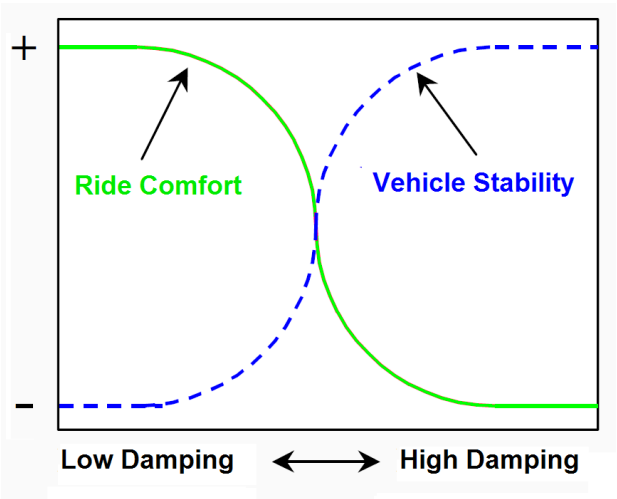

Figure 2.1: The compromise present in passive suspension design [5].

Even a good design for a passive suspension cannot give both performances at the same time, but also it can only optimize one set of the driving conditions by driver selection.

2.2 Adaptive Suspension

Refers to challenges were mentioned before, one of effective methods for suspension performance is capability of adaption between comfort and handling. The merit of adaptive suspension design is capability enhancement for different driving conditions. The suspensions adaptions are regulating damping number based of

driving condition, or adjusting suspension height based on driver set. These approaches can be done manually or by a set of suspension control unit.

2.2.1 Semi-Active

A good example for adaptive suspension which regulates damping number is a semi-active suspension system with adjustable shock absorber and Continuously Controlled Electronic Suspension (CES). Where the damping coefficients for each wheel are continuously adjusted in real time to ensure that the best compromise between comfort and stability is always achieved.

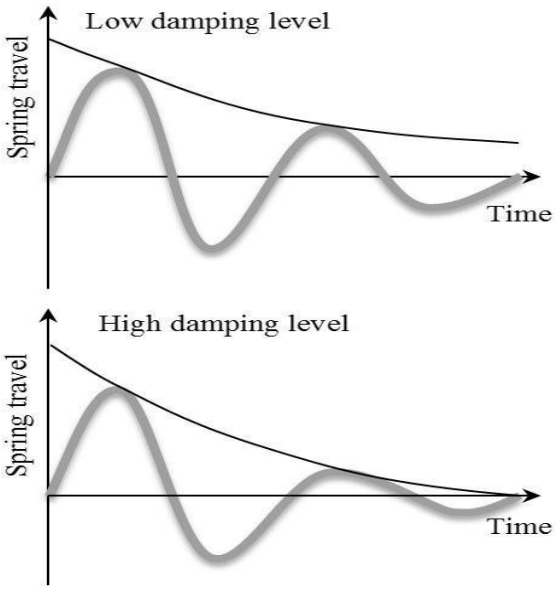

Figure 2.2: Spring travel for high damping and low damping level in Adjustable shock absorber.

2.3 Air-suspension

Another example for adaptive suspension based on suspension height or suspension with adjustable height is air-suspension. In this design suspension is using kinds of air-bag as spring. The vehicle height is adjustable based on driving condition for approaches such as vehicle stability by controlling vehicle's center of mass, and also height control in off-road driving.

Figure 2.3: Air-suspension height adjusts in a race care, increasing ride stability [13].

Figure 2.4: A sample of air-spring in air-suspension system.

2.4 Fully Active Suspension

The main difference in active suspension is its capability to inject force to the system. This force is generated by force actuators and it placed directly between wheel and body. In performing a control for an active suspension system, the time force function F (t) applies on the suspension system is show in fig.2.5 below.

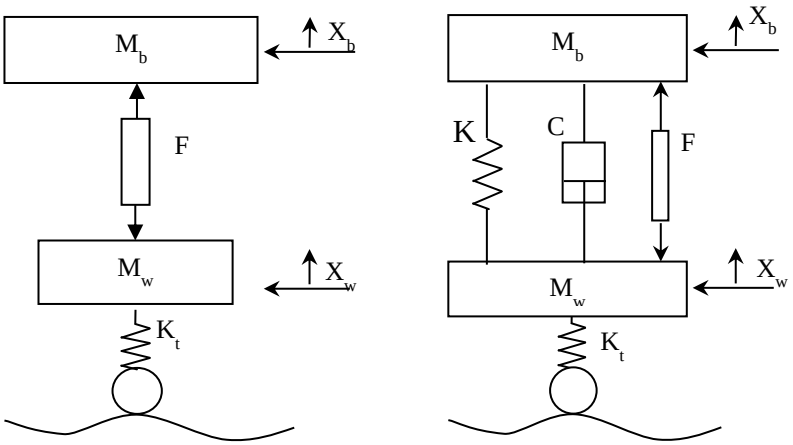

Figure 2.5: Diagrams of fully active and active suspension systems.

Normally the available actuators between wheel and body are spring and shock absorber. Active shock absorbers, Hydro-pneumatic Suspension and air-suspension are some examples for suspension with ability of activation against road disturbance. Linear Electromagnetic Suspension is a fully active suspension with rapid response against road irregularities. The main approach in active suspensions is obtaining terms of ride comfort and handling at once.

Figure 2.6: Bose suspension, an electromagnetic suspension [14].

In electromagnetic suspension, system properties are attained by a liner electromagnetic actuator. (Bose suspension)

2.5 Active Air-suspension

A typical model of a pneumatic active suspension can be modelled as a system consists of spring, passive damper, and a pneumatic active component. But the air-spring itself can play the role of both spring and pneumatic actuator. As it mentioned before, an active air-spring gives the opportunity of adjusting suspension ride height depend on road and vehicle condition. It can be used in load carrying, stance, tunability and handling. Considering air-spring as an actuator for force generation, requires real-time pressure control in air-spring chamber, which is called pneumatic Vibroisolation.

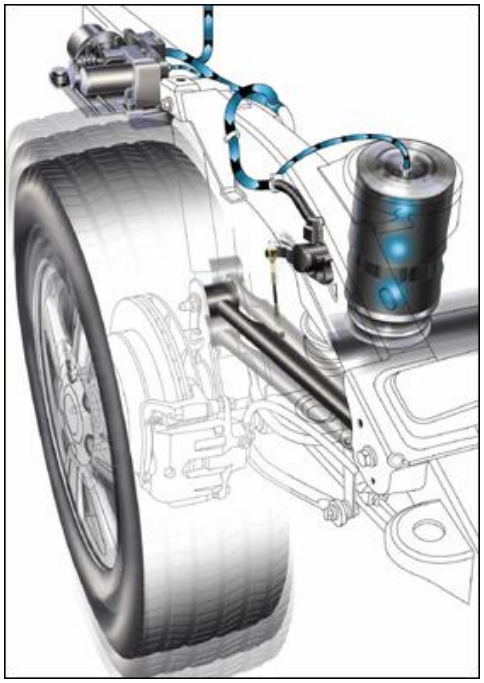

Figure 2.7: An active air-suspension system [15].

2.6 Pneumatic Vibroisolation

Pneumatic Vibroisolation is term of pneumatic control with the aim of ground vibration isolation. The main idea in this vibration control method is using a pneumatic chamber such as air spring, and vibration isolation can be done by pressure variation inside air-spring chamber. In this approach the controller is adjusting the air pressure with the aim of reducing acceleration in sprung mass. These pressure variations are applying by an air-valve, which is controlling the air flow inside the chamber.

Chapter 3

MODELING OF THE ACTIVE AIR-SUSPENSION

In this chapter a quarter-car suspension is modelled for experimental and simulation test in MATLAB-Simulink. First the physical structure and its mathematical equation will be present, then the actuator parts, control strategy and controllers will be explain.

3.1 Quarter-car Suspension Model

In this study a quarter-car model of an air-suspension is modelled as a system consisting of tire, wheel and body masses, air-spring and a shock-absorber as it shows below in fig.3.1.

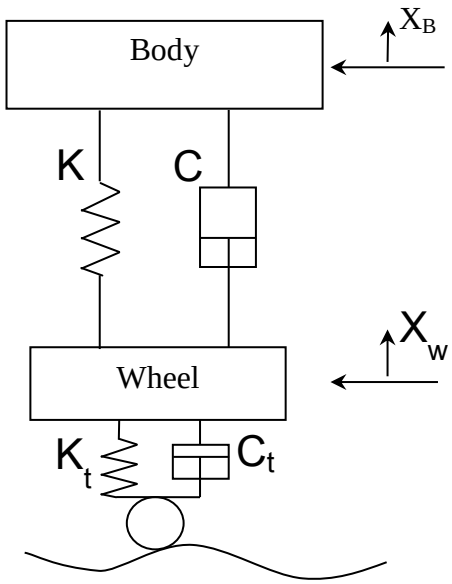

Figure 3.1: Schematic of quarter-car suspension model.

A physical structure of this model was prepared and its mathematical equations were modelled in MATLAB-Simulink. And also the air-spring and tire are modelled for simulation and experimental.

3.1.1 Physical Structure Model

The Physical structure was modelled, is a quarter of a passenger car in small size with the same ratio of real suspension system of a car.

It's a model consisting of a road simulator, tire, wheel, air-spring, a normal shock absorber and a mass considered as body.

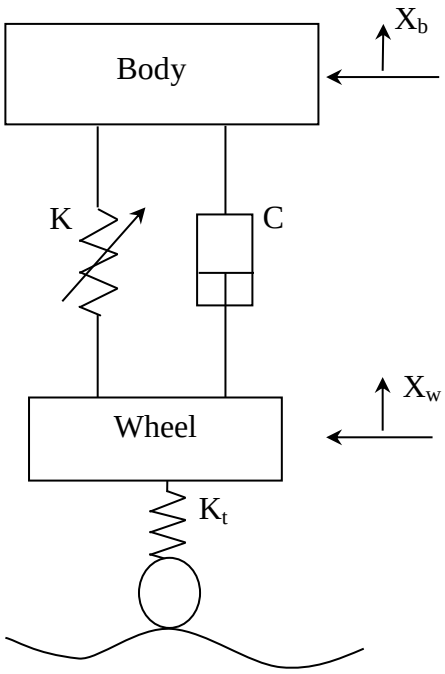

Figure 3.2: Schematic of quarter-car suspension model.

The new suspension system features, was experimentally modelled are shown below in the table 3.1.

Table 3.1: Properties and features of the physical structure

Mass of wheel (Kg)	36
Mass of body (Kg)	240
Stiffness of tire (N/m)	160000
Stiffness of air-spring in stable height (N/m)	16000
Damping number (Ns/m)	1400
Friction (N)	6
Gravity (m/s*2)	-9.8
Xb (m)	0.6
Xb, After gravity (m)	0.436
Xw (m)	0.2
Xw, After gravity (m)	0.183

3.1.2 Mathematical Model

The mathematical model used was a simple suspension operandi of a quarter-car, which simulates a linear model of spring in suspension system.

The equation 3.1 [1] is shown below was considered as the base of mathematical model.

$$M_b\ddot{x}_b = -C(\dot{x}_b - \dot{x}_w) - K(x_b - x_w) + u_c$$

$$M_w\ddot{x}_w = -\mathrm{C}(\dot{x}_w - \dot{x}_b) - \mathrm{K}(x_w - x_b) - K_t(x_w - r) - u_c \quad (3.1)$$

By considering gravity and parts position (road, wheel, body), the model was improved to equation 3.2 is shown below.

$$M_b\ddot{x}_b = -C(\dot{x}_b - \dot{x}_w) - K((x_b - h_b) - (x_w - h_w)) - M_b g + u_c$$

$$M_w\ddot{x}_w = -K(\dot{x}_w - \dot{x}_b) - K\big((x_w - h_w) - (x_b - h_b)\big)$$

$$-K_t\big((x_w - h_w) - r\,\big) - u_c \qquad (3.2)$$

The force-displacement diagram in a normal coil-spring is almost linear, however for air-spring, it's related to mechanical behavior of air inside a cylinder, and it's non-linear. The method used was real-time pressure sensing, and calculating stiffness from pressure inside the air-spring.

3.1.3 Simulink Model

The mathematical model of a suspension system was design in MATLAB-Simulink software and it's shown in fig.3.3 below.

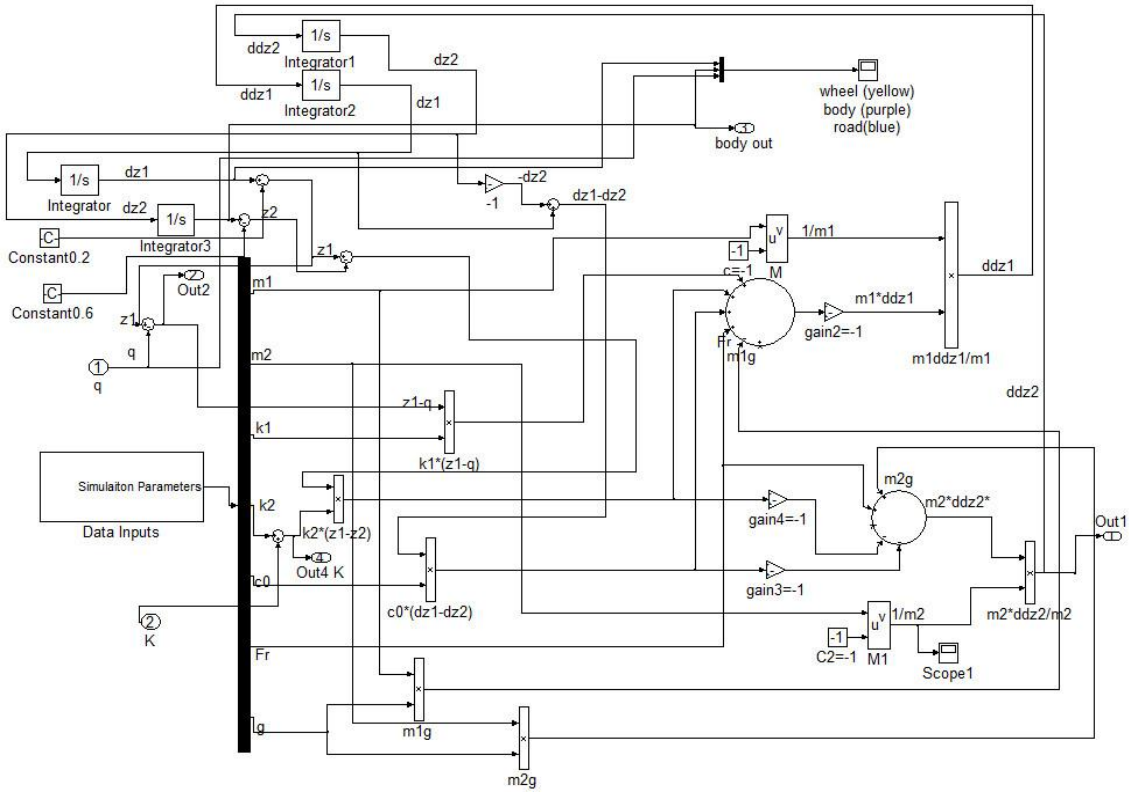

Figure 3.3: Simulink model of suspension equation, simulating passive suspension.

This suspension simulation diagram shows a passive suspension system is getting (q) as road and its simulating the position of wheel and body. Then it calculates the body acceleration and tire load to present suspension performance in comfort and stability.

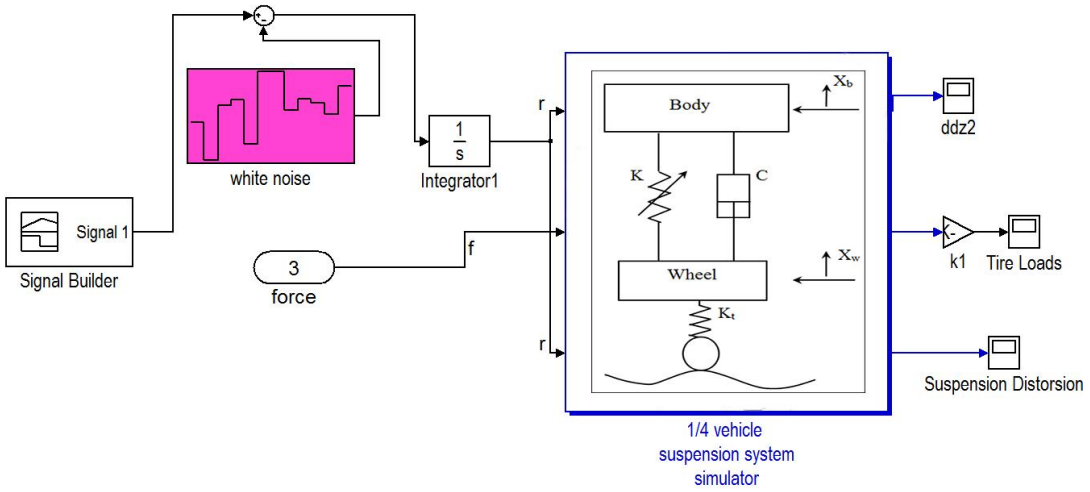

Figure 3.4: The Schematic of suspension simulation with force in MATLAB-Simulink.

Fig.3.4 shows a passive suspension with an external force added to the system. By the way it becomes active only if it receives the corrective force from a control system. The road disturbance was modeled for this simulation, is simulating a speed hump with a signal builder, and some noises are added to make it realistic.

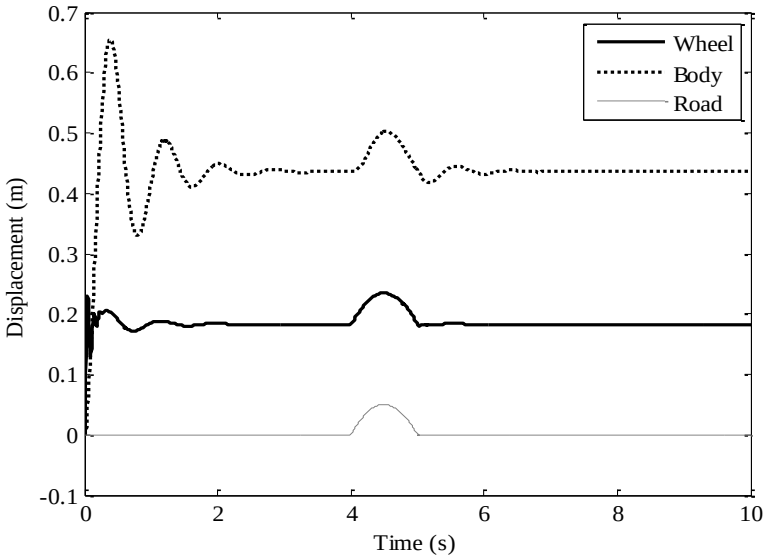

Figure 3.5: Diagram of wheel and body displacement passing a speed hump in passive suspension.

The fig.3.5 is shown above shows the simulation result for a passive suspension during passing a speed hump and this time it's without any noise. The wheel and body displacements in first 3 seconds are because of suspension parts positioning. By the beginning of simulation, wheel and body are going to be set in their given positions.

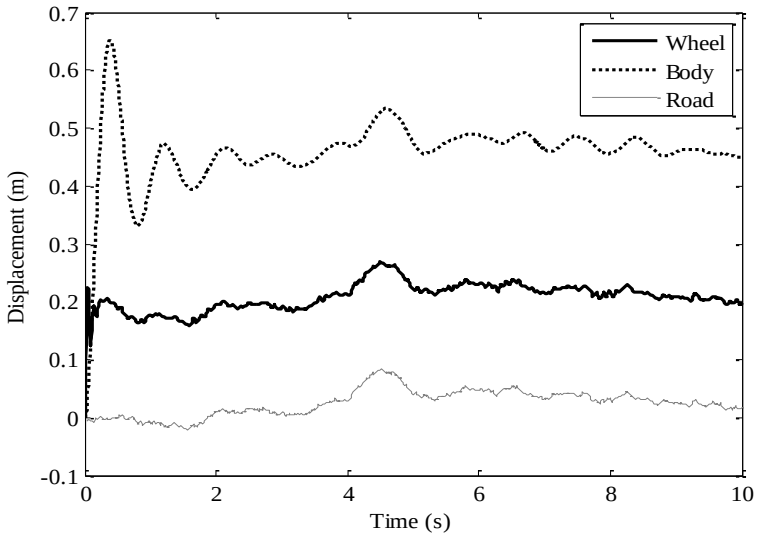

Figure 3.6: Diagram of wheel and body displacement passing a speed hump and noises in passive suspension.

Fig.3.6 shows the simulation result of a passive suspension for a speed hump and noises as road disturbance. The main control approach for active suspension is calculating the force which if it apply between wheel and body, it improves suspension performance in comfort and stability. In this study a model of force calculator was modeled in Simulink.

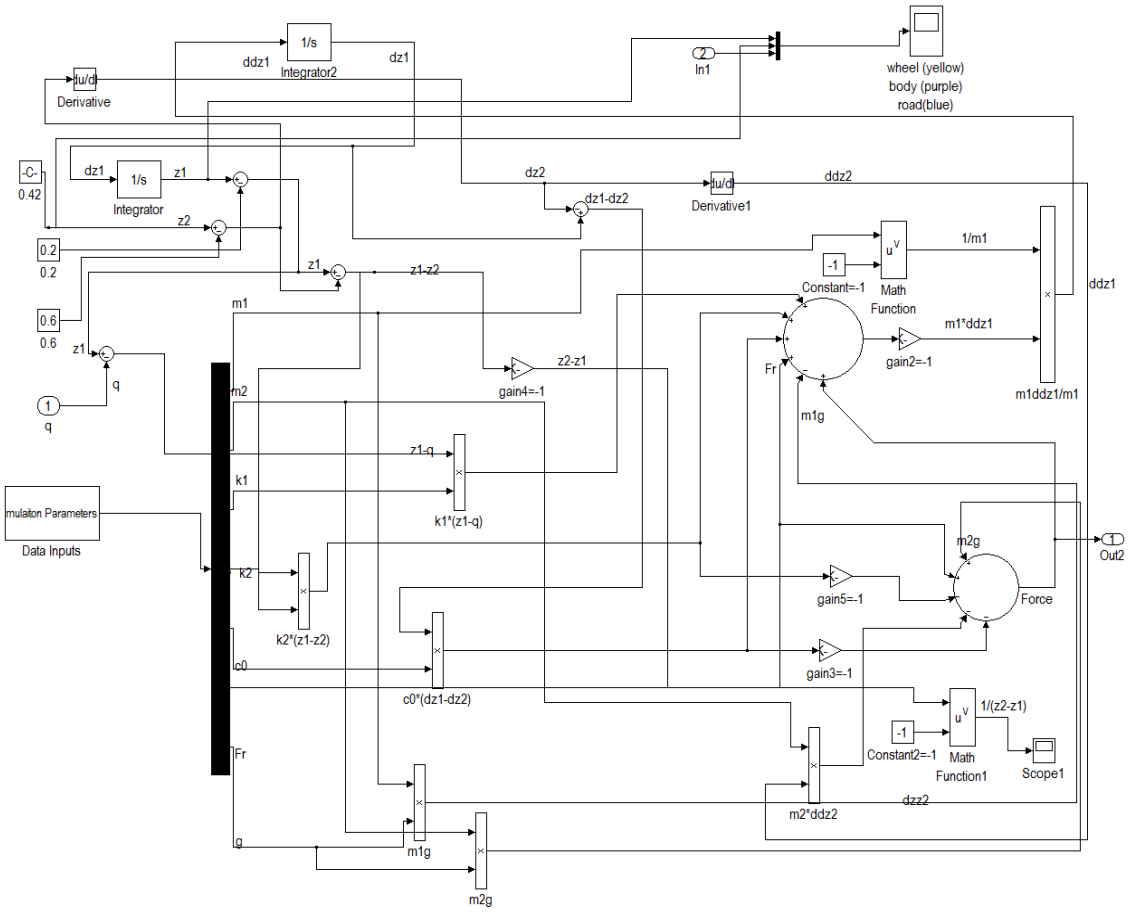

Figure 3.7: Simulink model of suspension equation is receiving suspension features and calculating force.

Fig.3.7 shows suspension equation which simulated in MATLAB-Simulink and used as force calculator. This equation is receiving suspension parameters as zero acceleration and displacement in body, and it calculate the external force, which if applied to system, the body acceleration will be zero.

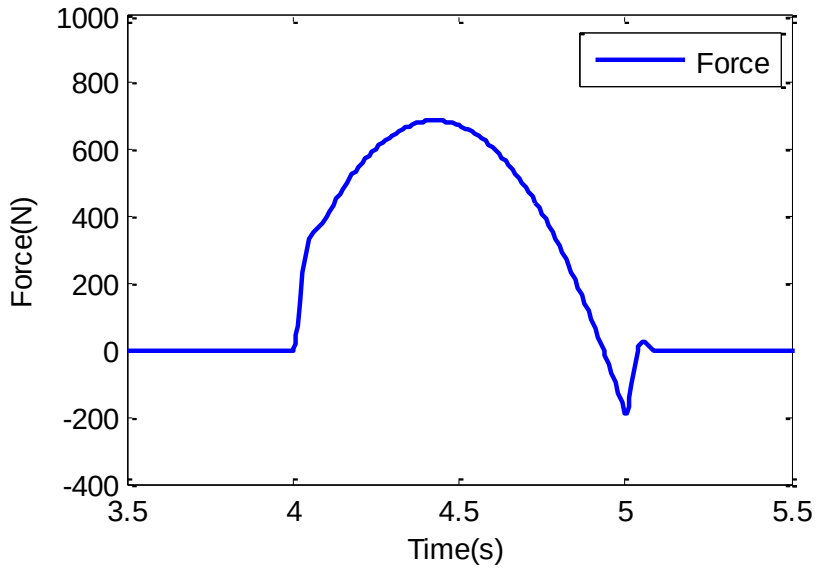

Figure 3.8: The force between wheel and body.

Fig.3.8 shows the force calculated from the equation was shown in fig.3.7.

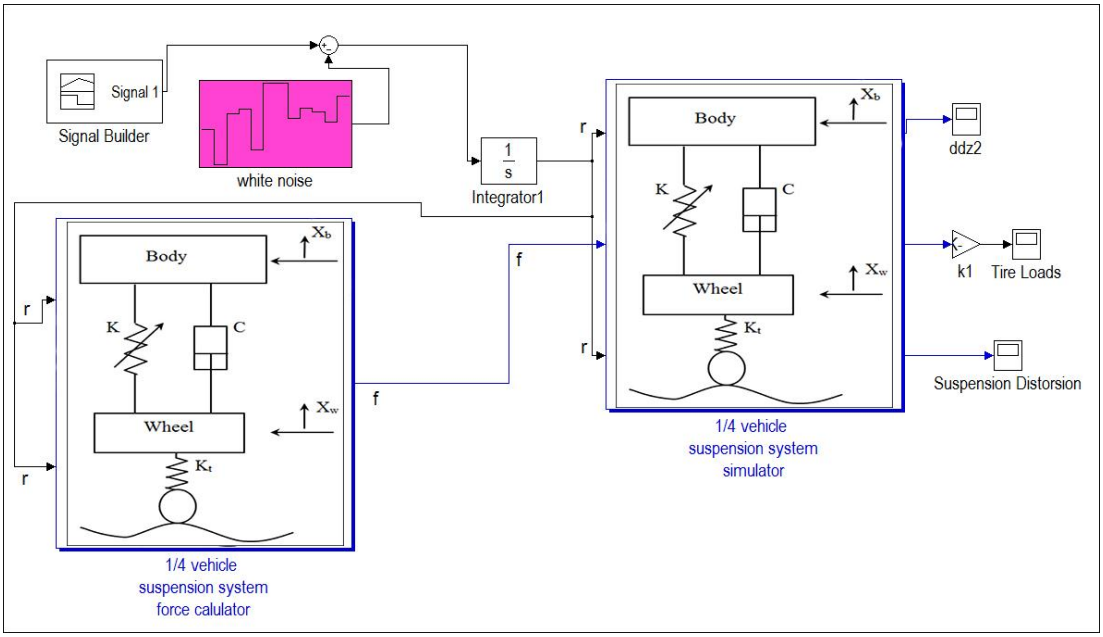

Figure 3.9: Schematic of active suspension simulation in MATLAB-Simulink.

Where, Fig.3.9 shows the quarter-car suspension simulation in MATLAB-Simulink.

The simulation model is simulating active components and suspension system. The control schematic is consisting of a force calculator and a suspension simulator. The first suspension model in left side is a calculator for activation orders. The mathematical model is used for this nonlinear suspension system is linear mathematical model and sensing the real time stiffness. And finally in right side three important results are displayed including body acceleration, tire load and suspension travel.

3.1.4 Non-linear Spring Model

Mechanical behaviour of gas inside a cylinder shows, stiffness of air-spring has non-linear relation between force and displacement. The way was used to get acceptable accuracy, was Stiffness calculation from real-time pressure sensing.

The mathematical equation for a quarter-car suspension Considering friction and gravity and position of wheel and body are shown below in equations 1 and 2.

$$M_b\ddot{x}_b = -C(\dot{x}_b - \dot{x}_w) - K\big((x_b - h_b) - (x_w - h_w)\big) + Fr + M_b g + u_c$$

$$M_w\ddot{x}_w = -C(\dot{x}_w - \dot{x}_b) - K\big((x_w - h_w) - (x_b - h_b)\big) - K_t\big((x_w - h_w) - r\big)$$

$$-Fr + M_w g - u_c \qquad (3.3)$$

The gas medium used in the air-spring is pressurized air; which is considered to be an ideal gas. The equation of state describing an ideal gas is known as Boyle-Gay Lussac's law [16]:

$$PV = m\,R\,T \qquad (3.4)$$

Where, P is the pressure, V is the volume, R is the specific gas constant, T is the absolute temperature and m the mass of air in the volume.

Boyle's law shows that in a constant temperature for a fixed mass, the pressure and the volume of a gas are inversely proportional.

$$P_1V_1 = P_2V_2 \tag{3.5}$$

$$F = \frac{(P_1V_1)A}{(x_2-x_1)A} \tag{3.6}$$

When F is the force generated in air-spring, p is the pressure of chamber, A is the affective area chamber, X_b and X_w here are the positions in tow side of chamber.

$$M_b\ddot{x}_b = -C(\dot{x}_b - \dot{x}_w) - (\frac{P_0V_0}{x_b-x_w}) + u_c$$

$$M_w\ddot{x}_w = -C(\dot{x}_w - \dot{x}_b) - (\frac{P_0V_0}{x_b-x_w}) - K_t((x_w - h_w) - r) - u_c \tag{3.7}$$

$P_0\ and\ V_0$ here are pressure and volume in stable height.

And also,$P_0V_0 = mRT$ so the parameter m is the mass of air and it can adjust related to air flow rat in air-valve. But, refer to datasheet of component; every air spring has its own force-pressure variation. For this air-spring the pressure-stiffness variation is following this equation [17].

$$K = a + bP - cP_2 \tag{3.8}$$

Where the k is rigidity of air spring (kN/mm) and P is gas pressure inside spring (Mpa).The multiples a, b, and c in the equation 3.3 was found for this air-spring is shown below in equation 3.4.

$$K = 0 + 0.6P - 0.5P_2 \quad (3.9)$$

By applying variation in pressure, the air-spring can adjust a suitable force to improve suspension performance [16].

$$P = F/A \quad (3.10)$$

Effective Area = (Load) kN / (pressure) kpa

3.1.5 Tire Model

One of effective factors in active suspension control is the tire and its suspension characteristics. It can be simulate a system consist of structural damping and the tire stiffness.

Figure 3.10: The tire model was used for the experiment.

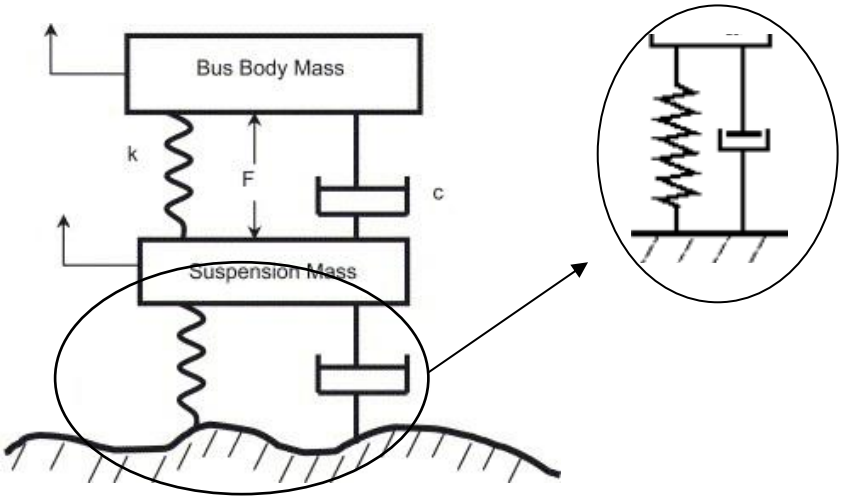

Figure 3.11: Schematic representation of the tire in suspension model [19].

So, the mathematical model of a tire is presented as [5]:

$$F_t = K_t(x_w - x_r) + C_t(\dot{x_w} - \dot{x_r}) \tag{3.11}$$

The road contact of the tire can be lost for a moment. In this case, the calculated tire force would be an impossible negative value. Because of this, a limitation is added to the first equation as follows:

$$(x_w - x_r) < 0 \longrightarrow F_t = 0 \tag{3.12}$$

3.2 Actuator Model

Getting similar result in simulation and experimental, requires high accuracy mathematical model in Simulation of actuators. Also simulation of pneumatic actuators plays an essential role for pneumatic muscle in robotic arms. In this section, air-spring and air valve will be introduced as pneumatic actuators in air-suspension system. First, actuators simulated were based on stiffness, and then actuators modelled based on pressure.

3.2.1 Stiffness Base Simulation

The first simulation attempt in this study for the control approach, was applying force to the system based on air-spring stiffness. And also the spring was modelled as normal linear spring.

Stiffness Variation Control

The main idea in this control strategy is based on stiffness variation, and a schematic of this control model is shown in fig.3.12 below.

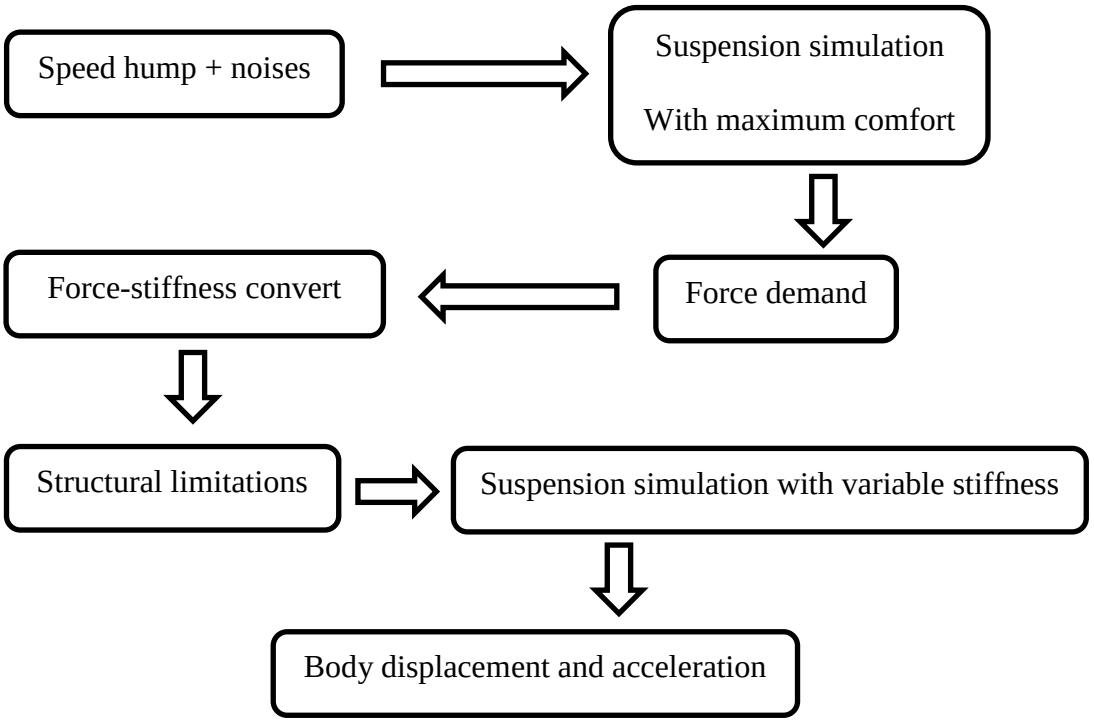

Figure 3.12: Schematic control strategy based on stiffness.

The force calculated from suspension equation was converted to stiffness. The structural limitations were considered before performing suspension simulator, and then it's comparing the results between active and passive. The stiffness is calculated from the force in this scenario; as such it is the approximate stiffness coming directly

from the force. And the simulation approach here is suspension behaviour analysis for stiffness variation.

Binary Orders

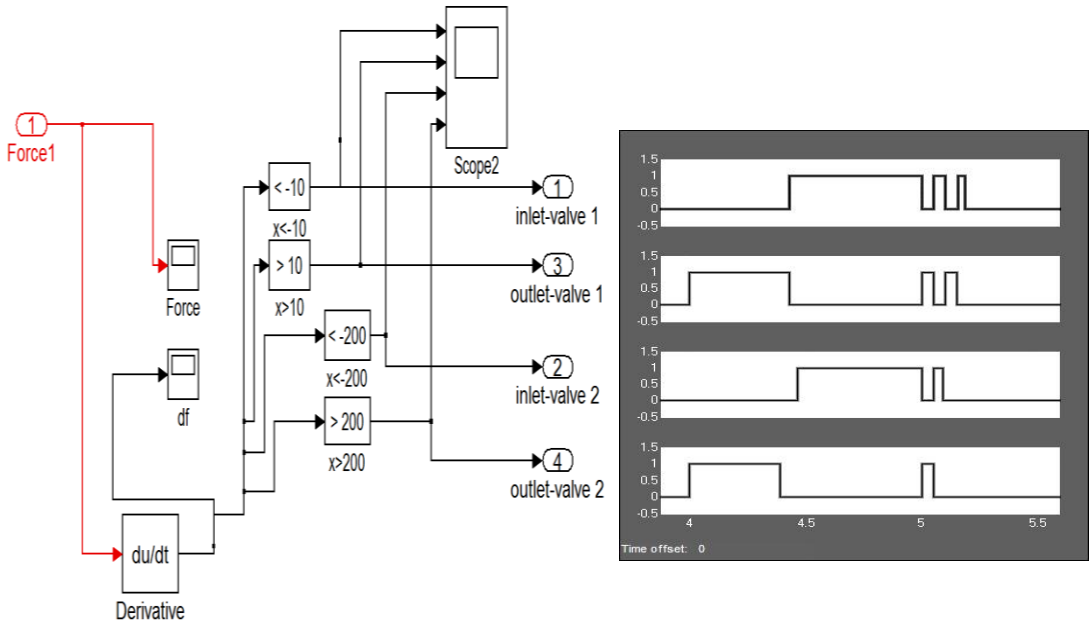

Figure 3.13: Diagram of binary orders for air-valves simulation.

Fig.3.14 shows a model, to find a binary order for solenoid-valves activation. Four air-valves are considered to control the air flow through the chamber. Inlet and outlet valves were used to charge and discharge the chamber, then second inlet and outlet valves were used for adjusting the flow rate into the chamber. The derivative of force shows, the speed of force variations, and control-orders are based on this speed. The speed of force variations above and below 10 N/s is activating inlet and outlet valves; by the way it applies a force through the correct direction. Second valves were designed to be activated only if the speed of force variation is above or below 200 N/s. This model used was for experimental control approach and, numbers 100 and 200 here should acquire experimentally. And the model can be integrated with

simulation and experimental results comparison in a neural network based on real-time estimation of perturbation signals.

Air-valve Activation

The air-valve was simulated in two segments of electric solenoid and flow throttle. And its control schematic in Simulink is shown below.

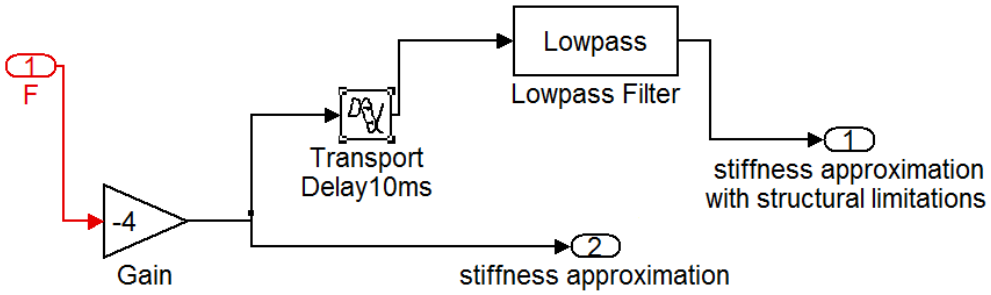

Figure 3.14: Simulink model of stiffness simulation from the force.

The gain -4 in this model is converting force unit to stiffness. This method used to show the effect of stiffness variation in body displacement. The low-pass filter used was simulating the lag of air-spring and the delay used was simulating electric solenoid delay.

Simulation Development

The schematic of integrated control system is shown below in fig.3.15.

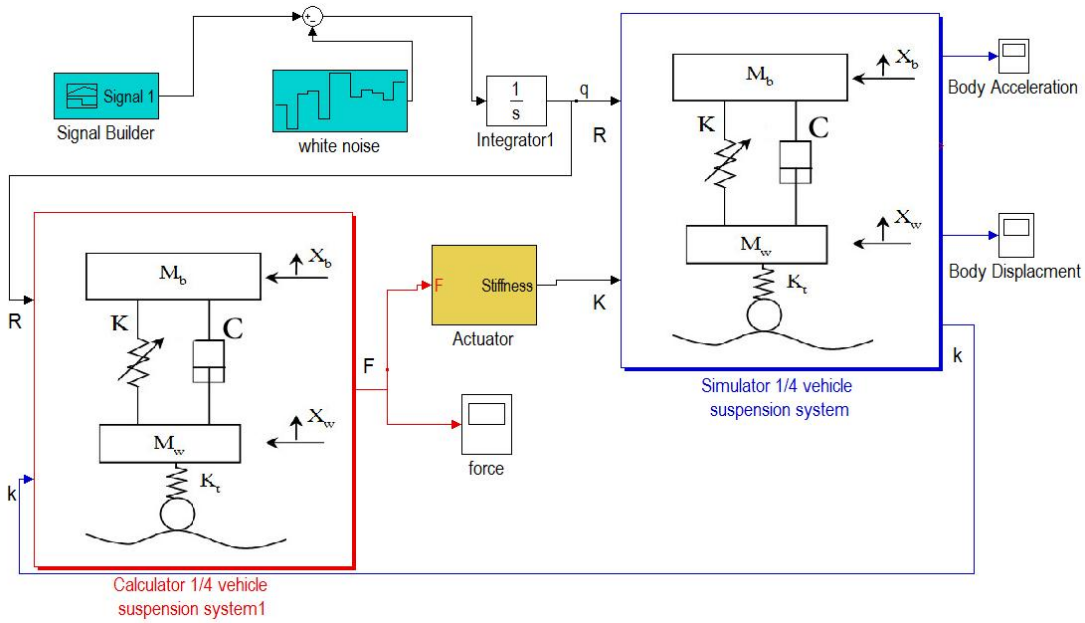

Figure 3.15: Schematic of control model in MATLAB-Simulink.

3.2.2 Pressure Based Simulation

Whereas air-spring activation is based on pressure, the final experimental and simulation model were designed based on pressure inside the air-spring.

$$M_b\ddot{x}_b = -C(\dot{x}_b - \dot{x}_w) - (0.6P - 0.5P_2)(x_b - x_w) + Fr + M_b g + PA$$

$$M_w\ddot{x}_w = -C(\dot{x}_w - \dot{x}_b) - (0.6P - 0.5P_2)(x_w - x_b) - K_t(x_w - r) - Fr + M_w g - PA \quad (3.13)$$

A desired model with 100% performance in comfort and handling was designed in Simulink to calculate the desired force and then the pressure for air spring, from the equation was mentioned before ($u_c = PA$) . The model was considered with no motion in body and also without tire deflection, so;

$K_t(x_w - r) = (M_{total})g = constant \rightarrow r = x_w \rightarrow 100\%\ stability$

$x_b = contant \rightarrow \dot{x_b} = 0 \rightarrow \ddot{x_b} = 0 \rightarrow 100\%$ comfort

Then the pressure calculator equation without considering friction is;

$$0 = -C(\dot{x_r}) - (0.6P\ -\ 0.5P^2)(r) + M_b g + u_c$$

$$M_w \ddot{x_r} = -C_p(\dot{x_r}) - (0.6P\ -\ 0.5P_2)(r) - (M_{total})g + M_w g - u_c \qquad (3.14)$$

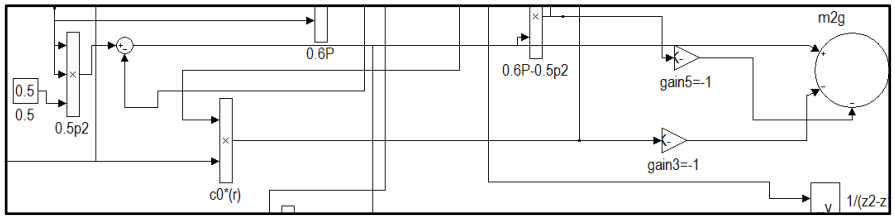

Figure 3.16: A schematic in Simulink, Calculating pressure part in air suspension equation.

For this simulation the method used was converting force to pressure, after calculating force from suspension equation.

3.2.3 Air-spring Model

In the Pneumatic spring modelling, the force generated by a pneumatic cylinder can be written as:

$$F = (P - Pa)\ A \qquad (3.15)$$

Where P is the gas pressure within chamber, and A denote the effective working area of chamber. Due to Lussac's law was mentioned before, the relation between pressure and the amount of air inside air-spring is; $m = \frac{PV}{RT}$ then the pressures in the chamber and the capacity will be derived. Thus, the pressure gradients in the chamber can be derived similarly. Since the control system is based on pressure variation in constant volume, gas volumes within the air-spring is constant. In other hand, air-spring activation is performing by air valve, and pressure variation will be the result of air-flow and its flow rate within chamber.

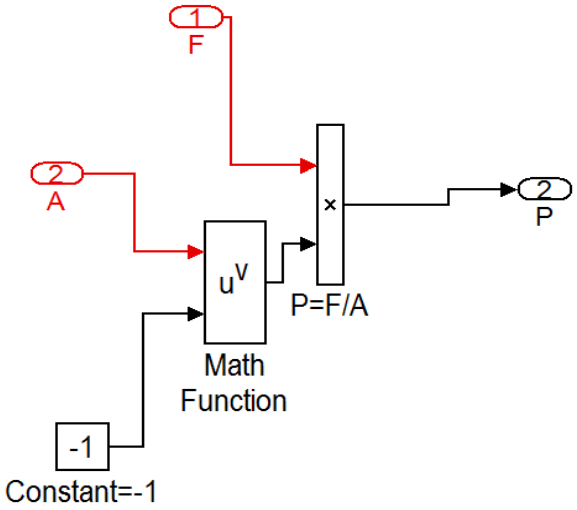

Figure 3.17: A schematic in Simulink, Calculating pressure from the force.

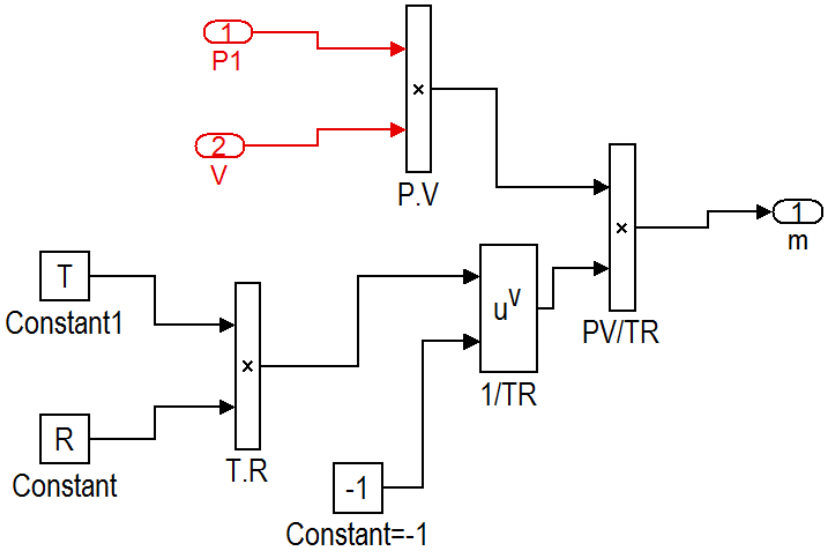

Figure 3.18: A schematic in Simulink, Calculating amount of air

3.2.4 Air-valve Model

A 5/3 solenoid air-valve was used for adjusting amount of air inside the chamber. The features of the valve used are shown below and it helps to find solenoid delay or response time. The solenoid valve part was modelled with a delay.

Figure 3.19: The pneumatic air-valve used for exprimental study.

The second segment for air-valve was modelling of throttle in air flow rate for different pressures. A part of valve datasheet related to throttle is shown below in fig.3.17

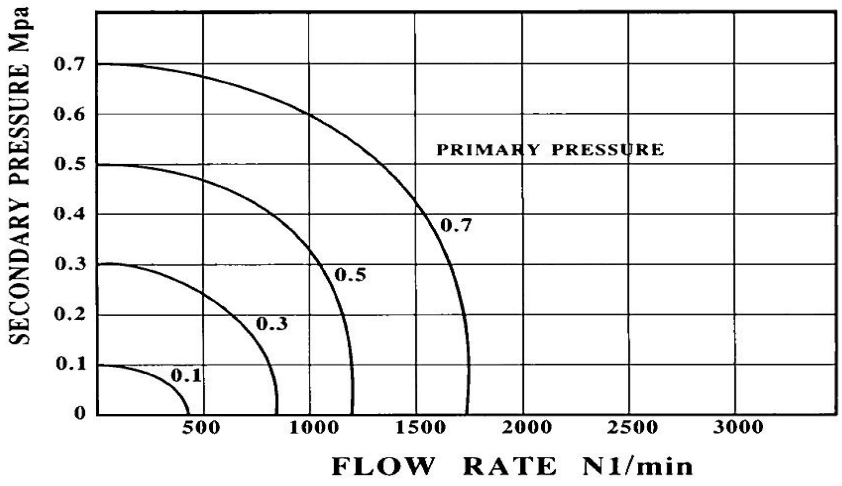

Figure 3.20: diagram of flow rate in different pressures, the flow feature part of air-valve detasheet [20].

In this level, flow rate and amount of air ($m\ and\ \dot{m}$) which was requested from calculator is compared with amount of actual air in chamber and the ability of flow rate from air-valve. Here are two different conditions to activate air valve. If the flow rate requested from calculator is bigger than flow rate ability in air valve, the moment, program activates the valve. If the flow rate requested from calculator part is less than capability of air valve for air flow, the program compare amount of desired air with amount of actual air inside the chamber.

The solenoid part here has 50ms delay to open the throttle, and amount of air variation after opening the throttle is flow rate multiply with time ($\dot{m}t$),so;

$$\Delta m = \dot{m}t \tag{3.16}$$

The time in equation (3.16) is duration of air valve activation. If this duration is more than 50ms (delay in solenoid), program activates the valve due to duration calculated.

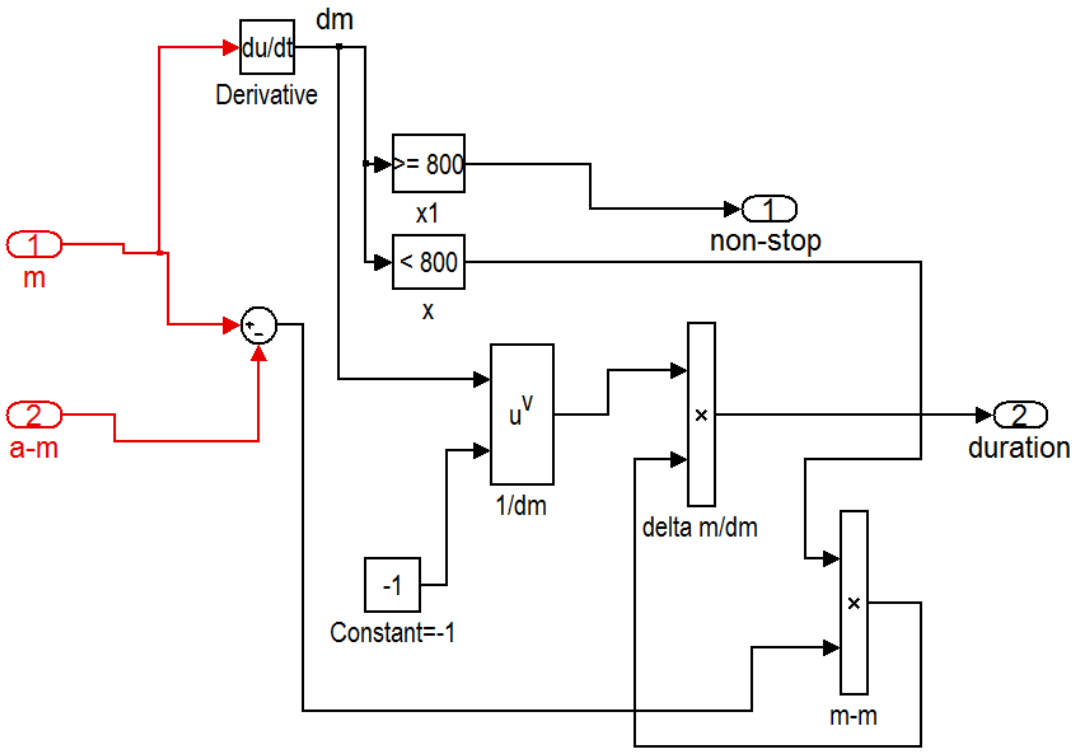

Figure 3.21: The control schematic for valves activation in simulink.

3.3 Control Strategy

This study proposed a control scheme based on real-time pressure estimation for active nonlinear suspension systems in unknown excitations due to irregular road surfaces. The approach differs from other active suspensions because the control strategy is designed based on pneumatic vibration isolation in conjunction with a linear spring and time varying stiffness was modelled as nonlinear spring. The suspension dynamic mathematical model is only requiring position pressure measurement. The schematic of control strategy is shown below in fig.3.16.

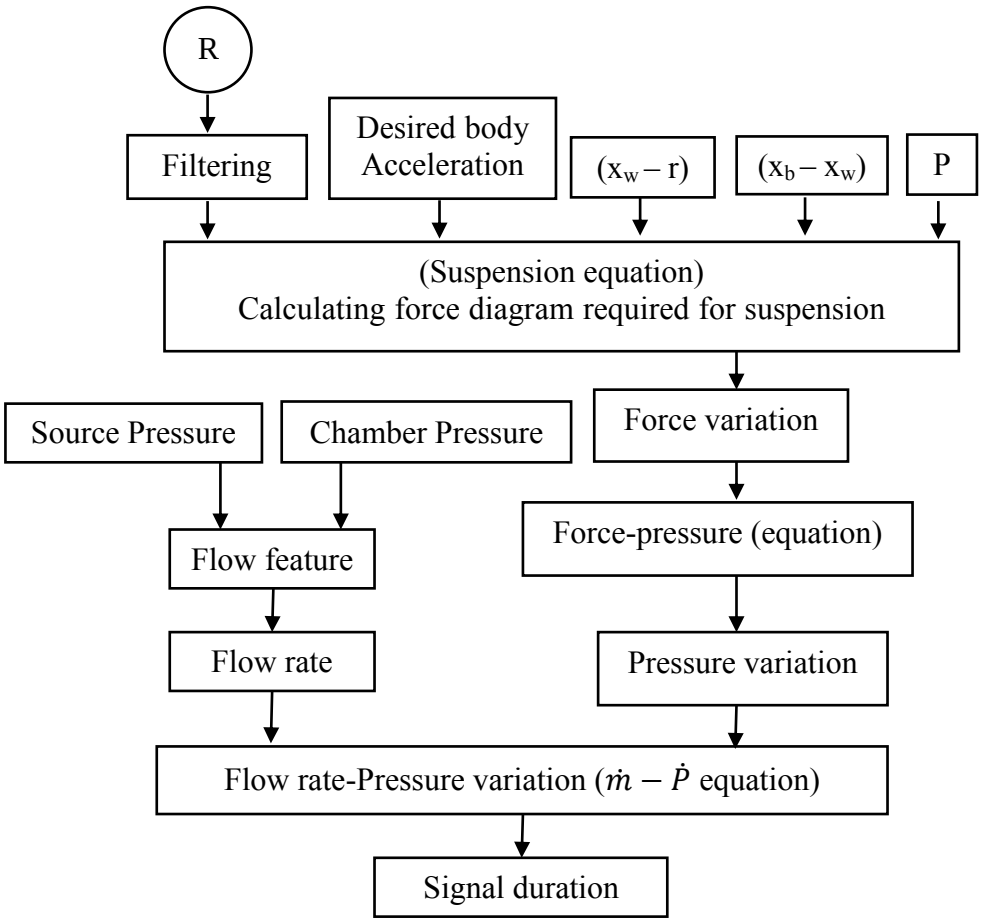

Figure 3.22: Schematic of control strategy for experimental model.

For every step data's were compared with the chamber pressure to get feedback from the control model. Bay the way it's a close loop control model passed on pressure.

3.4 Experimental Model

For the experimental approach, a model was developed and used for results validation survey. The controller hardware's and software will be explained in this part. The feature for this physical structure of model includes body, tire, wheel, air-spring and damper are presented in table 3.2 below. This model was installed on a road simulator which is working independently and simulating speed hump.

Table 3.2: Features of physical structures for the experimental model.

Mass of wheel (Kg)	6
Mass of body (Kg)	35
Stiffness of tire (N/m)	50000
Stiffness of air-spring in stable height (N/m)	6000
Damping number (Ns/m)	160
Friction (N)	4
Gravity (m/s*2)	-9.8

The air-spring selected in this approach was belongs to a truck cabin suspension is shown below in fig.3.23.

Figure 3.23: Air-spring used for experimental model [21].

3.4.1 Controller Hardware

The control hardware consisting of sensors, interface board, data acquisition card and electronic relay system was design to apply the control strategy in experimental model.

Position Sensors

The position sensor used in this experimental study was flex sensor. Flex sensor normally is used for Angle Displacement Measurement, and its sensitivity is its body deflection. In this case it was used as a height sensor and linear displacement was mechanically converted to angular by help of constant force spring. The flex sensor was installed on a spring tape and 2 side of tape were screwed to tow different parts. The length of this spring tape is the number can specify the relation between resistance and displacement.

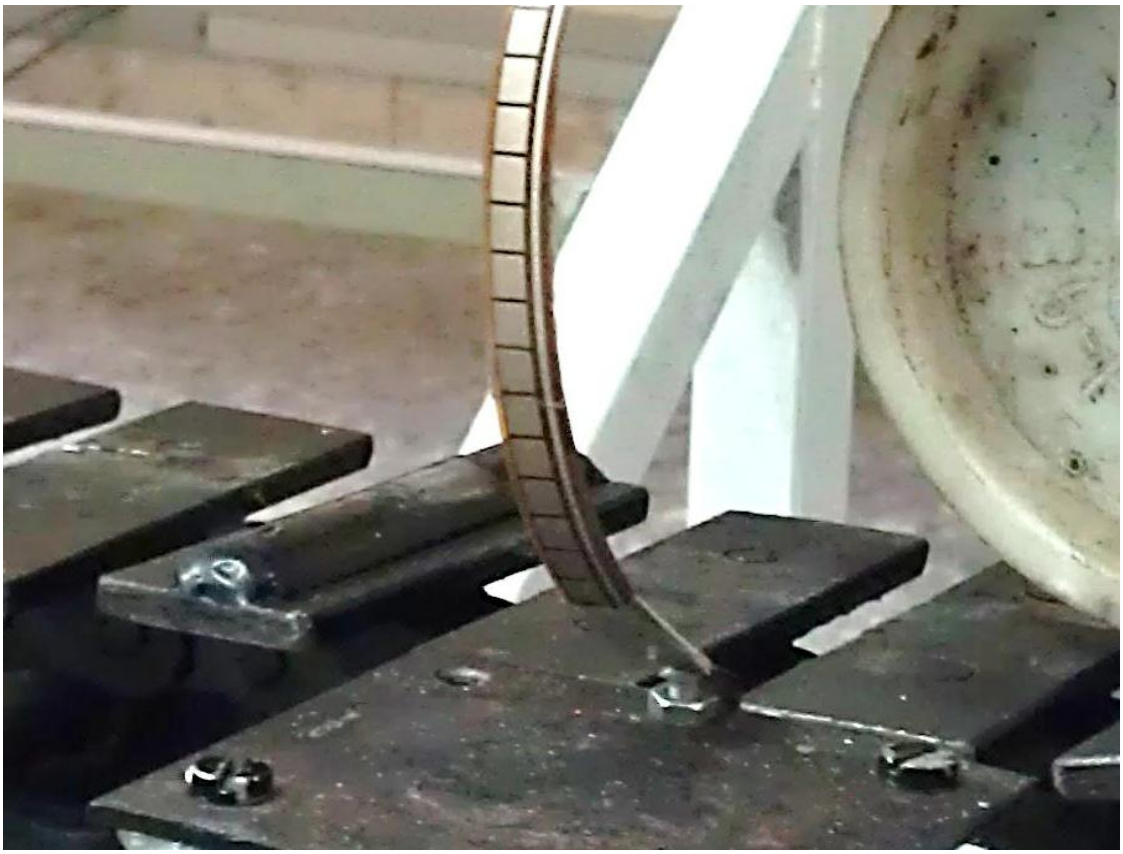

Figure 3.24: Flex sensor used for experimental model.

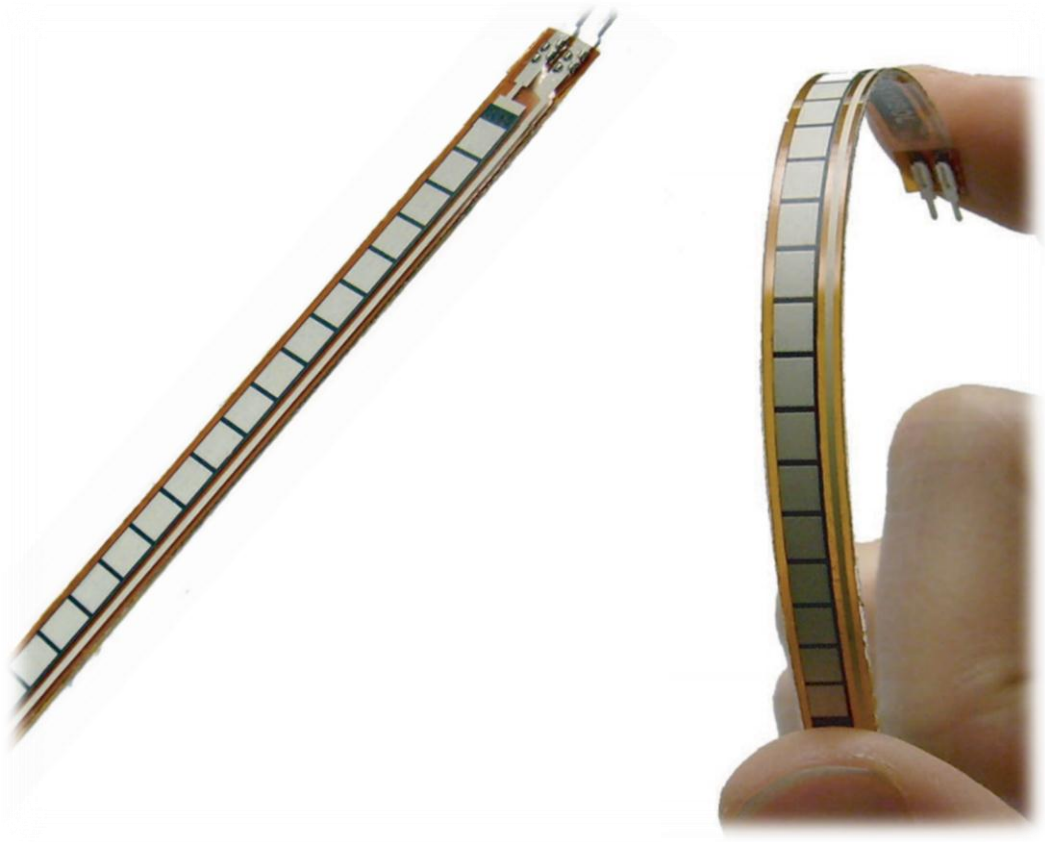

Figure 3.25: Undeflected and deflected flex sensor [18].

Specifications

- Life cycle: >1 million
- Height: ≤ 0.43mm (0.017")
- Temperature range: -35°C to +80°C
- Flat resistance: 10KΩ
- Resistance tolerance: ±30%

The output data from flex sensor is resistance variation, and the DAQ card can only sense voltage variation and convert it to displacement. An electronic interface board was designed for converting resistance to voltage.

Pressure Sensor

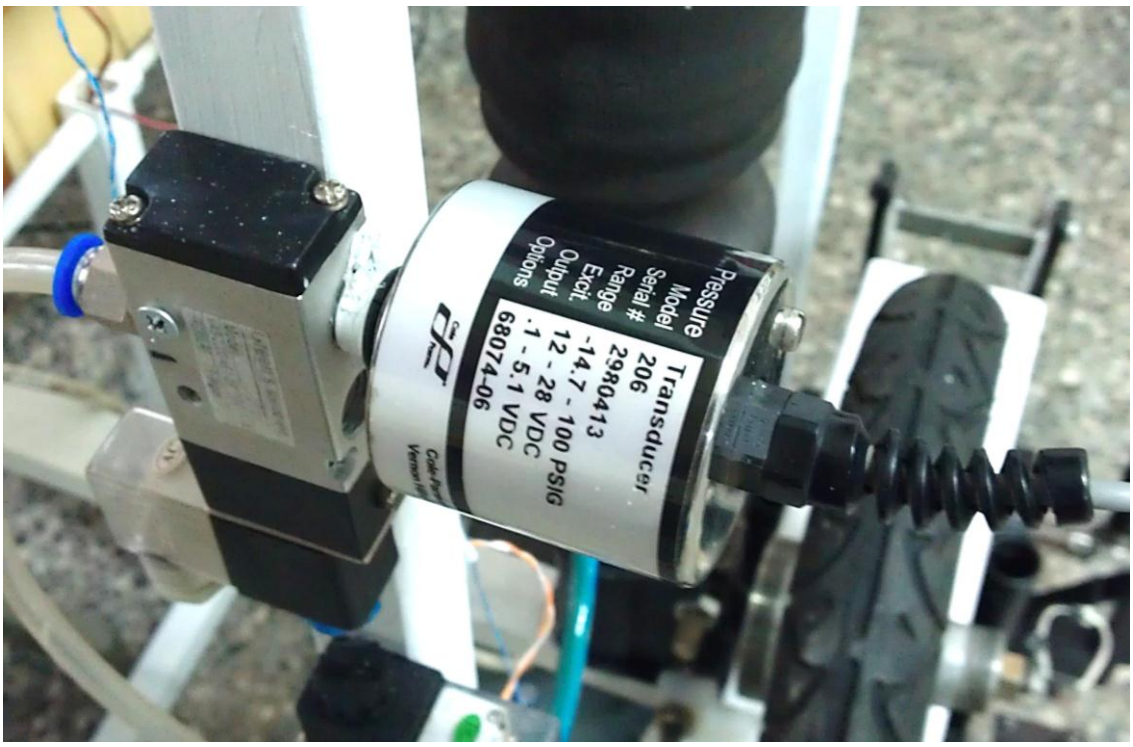

Figure 3.26: pressure sensor used in the experimental model.

The pressure sensor was selected for this study is in high accuracy to implement the chamber pressure during control processes. This sensor was giving data's by voltage variation; by the way it can connect directly to DAQ card and shows the pressure from -14 up to 100psi by voltage variation between 0.1 up to 5.1 volt.

Specifications

- Range: -14.7 to 100 psi
- Output: 0.1 to 5.1 V
- Power: 12 to 28 VDC (unregulated)
- Accuracy: ±0.13% full-scale

Interface Board

Interface board is a device between computer in one side and sensors and actuators in other side. A control board was prepared to supply sensors and adjustable to set the zero point for sensors. Fig.3.26 and fig.3.27 are showing interface board used for experimental model.

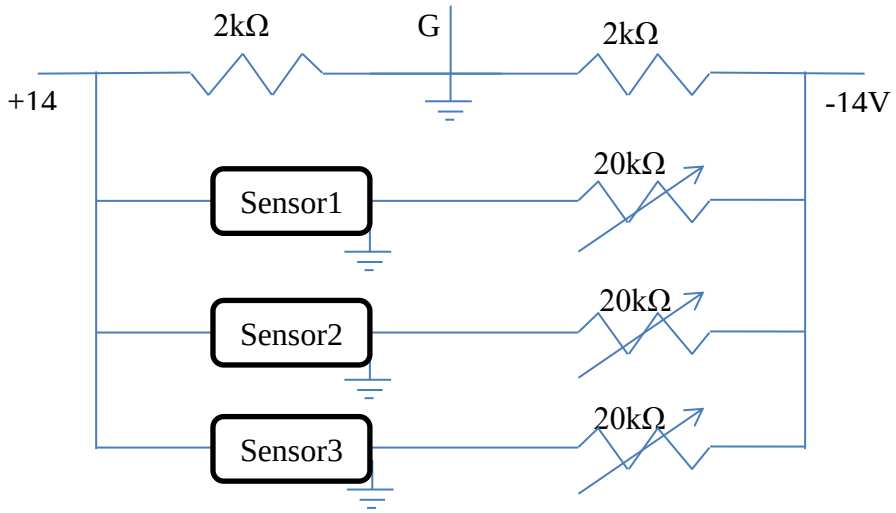

Figure 3.27: Schematic of electronic board, converting resistance to voltage.

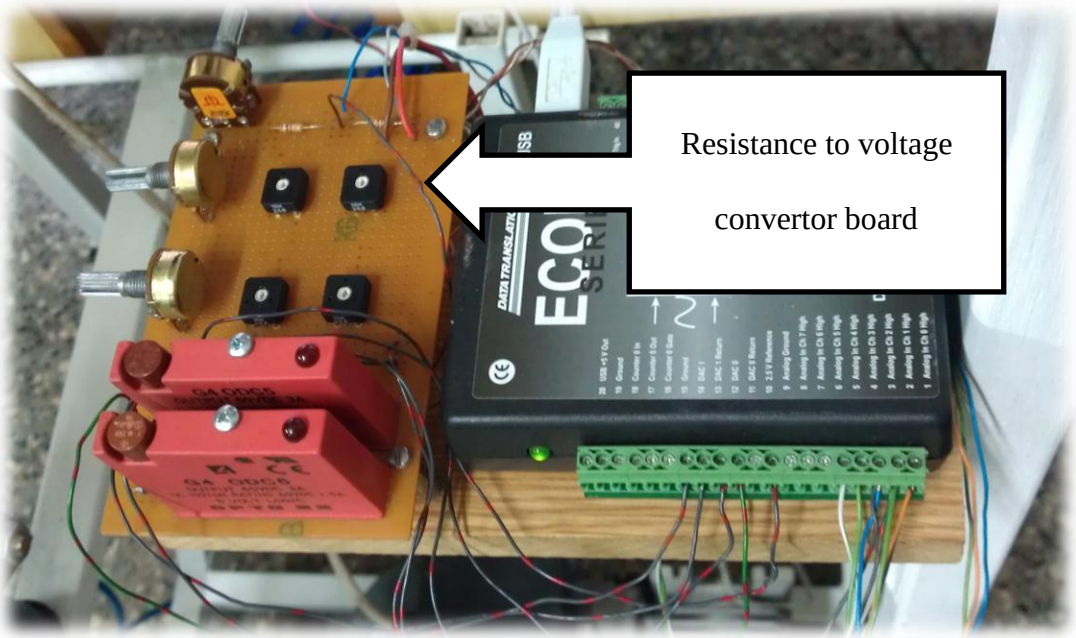

Figure 3.28: interface board include solid relay, convertor and DAQ card.

Data Acquisition Card

A USB data acquisition card was selected for the experimental part of this study the DAQ card used, was a .DT9812 from data translation with 8 Analog inputs, 2 ports for digital input and 4 Analog outputs. 3 position sensors and one pressure sensor were connected to Analog input ports from zero to three.

Figure 3.29: DAQ card used in the experimental study.

Electronic Relay System

The time and delay has significant role for active suspension control, as is mentioned before about TDC control method, every delay should be calculated in control system, and also it has negative effect on active suspension performance. Solid relay with less than one millisecond delay were used to decrease delay time in activation part. Fig.3.27 shows the solid rely used for experimental of this study.

Figure 3.30: The solid relay used in the experimental study.

3.4.2 Controller Software

The experimental model was run with Lab-VIEW software to perform the control strategy on the suspension system.

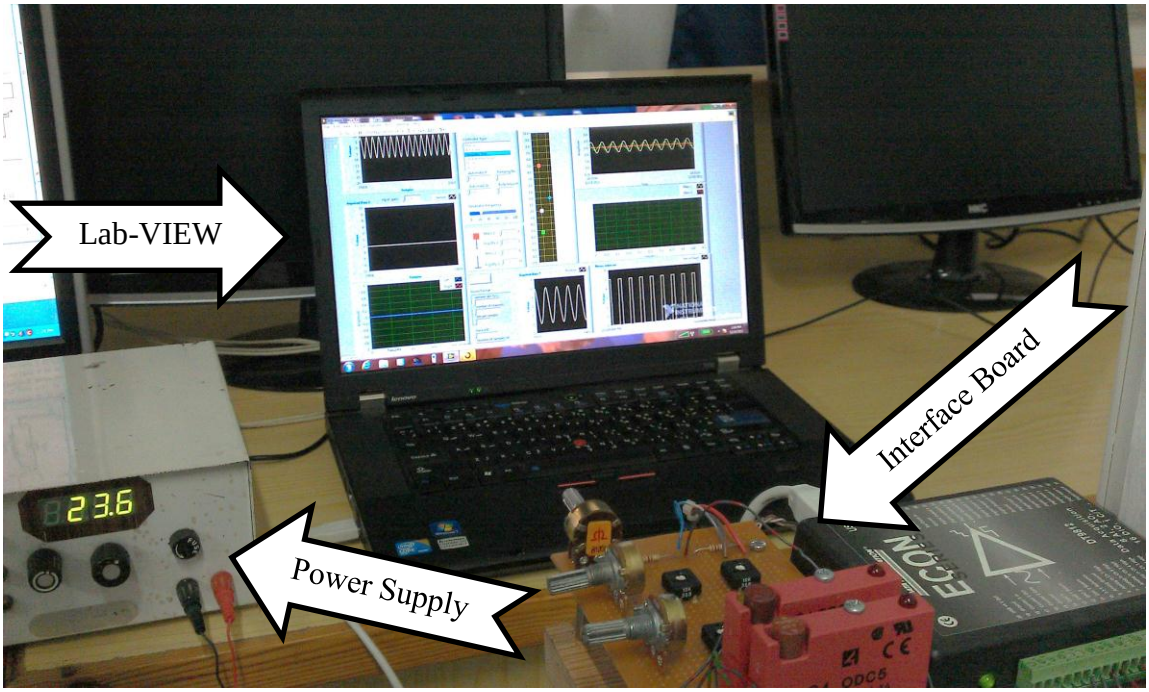

Figure 3.31: Controllers.

A control model similar to the model in Simulink was prepared to receive data's from height sensors and pressure sensor, and control solenoid valves for approach of suspension performance improvement.

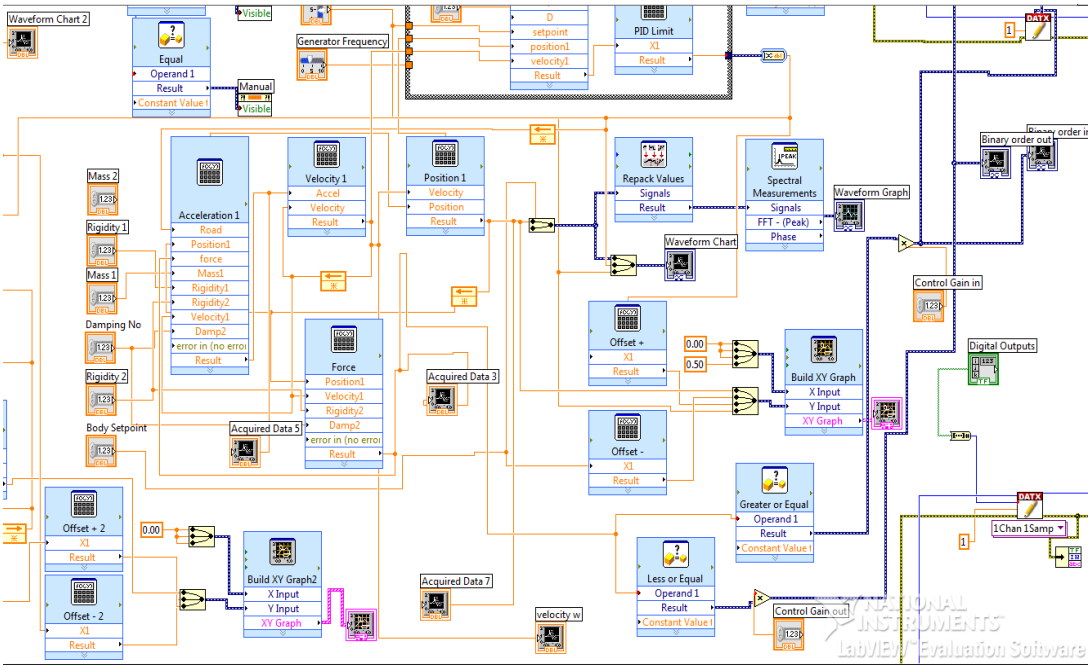

Figure 3.32: Controller, Lab-VIEW Block diagram in experimental study.

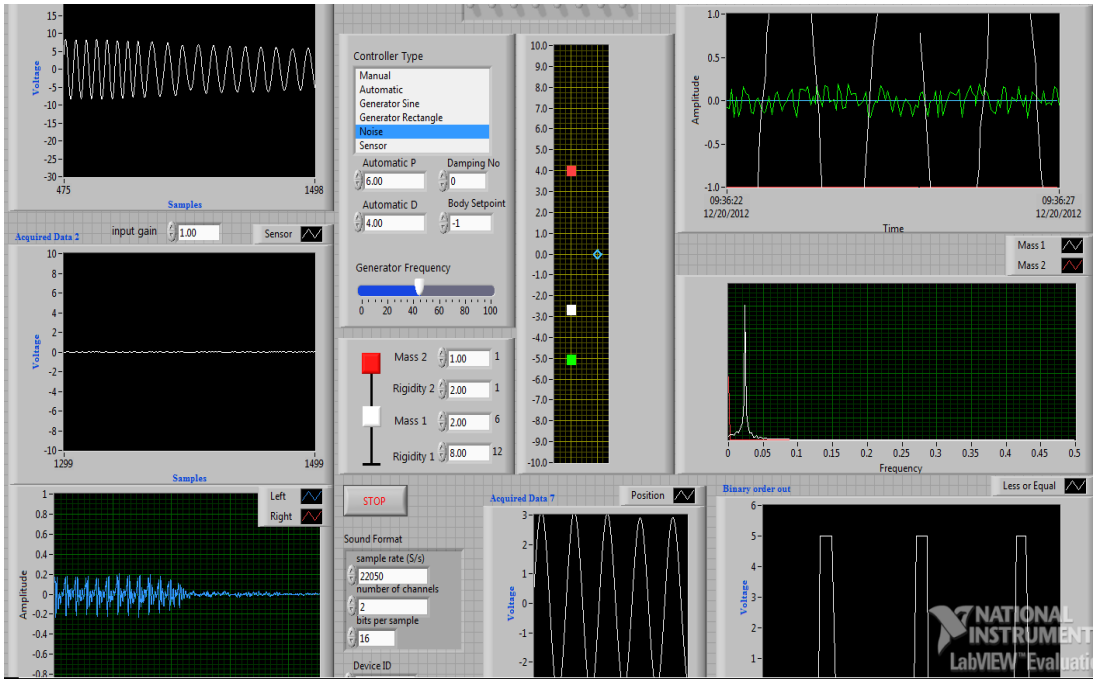

Figure 3.33: Controller, Lab-VIEW Front panel in experimental study.

When the program rune the model, it measures input road from road simulator, it also sense the deflection in tire and it sense the suspension travel directly from position sensors. Suspension travel sensor can also help to calculate capacity of chamber. The pressure sensor presents the real time pressure inside the chamber. So it helps to calculate amount of air inside the chamber and momentary stiffness.

Chapter 4

SIMULATION AND EXPERIMENTAL TEST RESULTS

In this chapter the accuracy of experimental study will evaluate, and the performance of new suspension for simulation and experimental will be calculate in tow approach of comfort and stability, to evaluate the new suspension performance. In the new suspension, comparisons with the passive suspension clearly demonstrate the superior performance of the active air-spring.

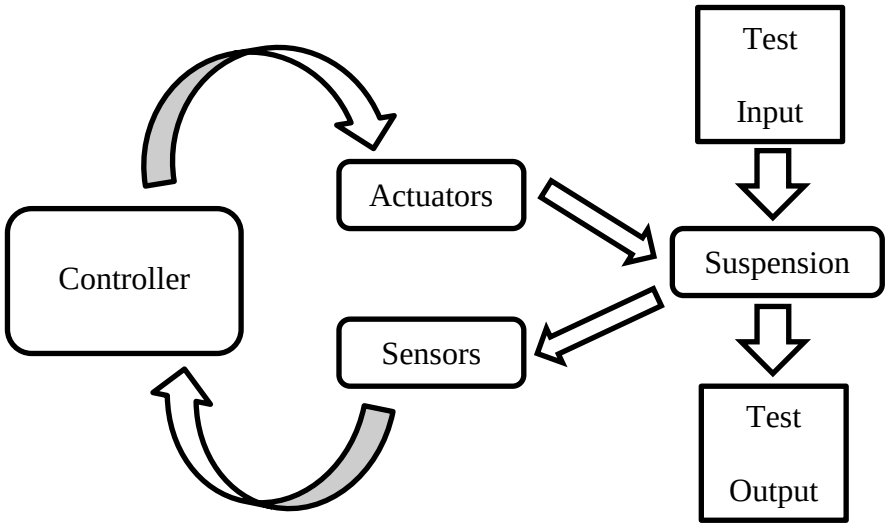

Figure 4.1: Schematic of test design for experimental study.

4.1 Model Validation

The accuracy of experimental study presents the validation of this model. This part explains about evaluation of results similarity between experimental and simulation in order to specify the percentage of model validation.

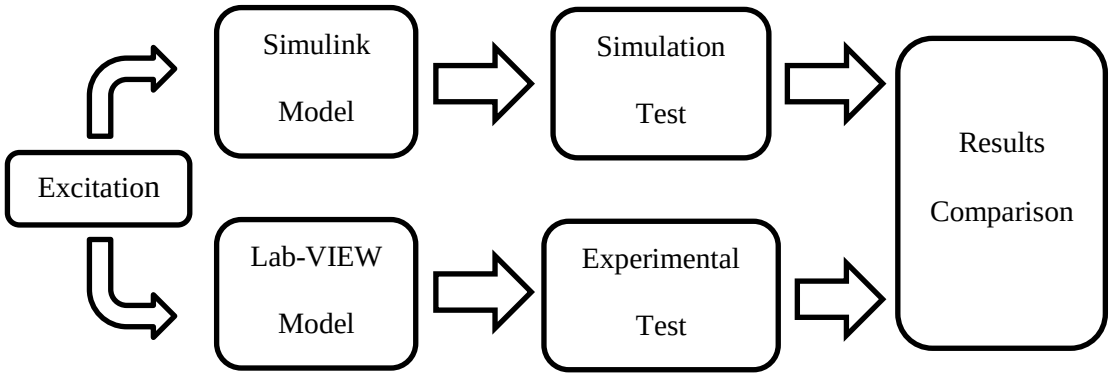

Figure 4.2: Schematic of validation evaluation design for this study.

Result comparison between simulation and experimental requires a data reduction in order to analyse the magnitude characteristic of a data series. RMS or root-mean-square is the most common method for amplitude of a set of data expression. It presence the average of data magnitude, and also it can indicate the vibration energy. The mathematical formulation to define RMS is shown in equation (4.1) [5] below.

$$[t, a(t)] \rightarrow RMS(a) = \sqrt{\frac{1}{T}\int_0^T a^2(t)dt} \tag{4.1}$$

And the partible formulation can be defined as:

$$RMS = \frac{\sqrt{({a_1}^2 + {a_2}^2 + \cdots + {a_n}^2)}}{n} \tag{4.2}$$

For example the fig.4.3 has shown below presents the experimental passive tire deflection. Tire deflection is selected to show RMS calculation method in order to evaluate the suspension stability.

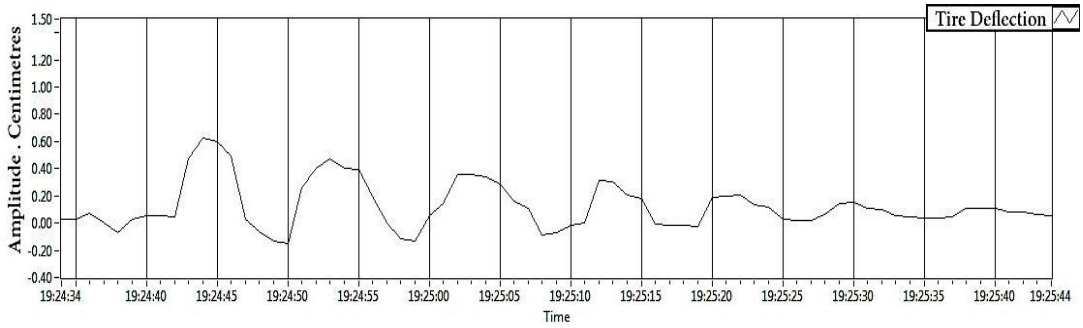

Figure 4.3: Diagram of tire deflection in passive experimental test.

In fig.4.3 there are vertical lines for every five milliseconds in the diagram. Considering more vertical lines gives more accuracy to define RMS number. The number of vertical lines in this study is for every one millisecond.

Average Values and the Standard Deviation

The general formula for calculation of the average value X_{AV} (sometimes also called mean value) is as follows:

$$X_{AV} = \frac{1}{n}(x_1 + x_2 + x_3 + \cdots + x_n) \tag{4.3}$$

Where n is the number of repeated measurements. The values of the deviation from the average value are used to calculate the experimental error. The quantity that is used to estimate these deviations is known as the standard deviation s_x and is defined as:

$$S_x = \sqrt{\frac{1}{n-1}[(x_1 - x_{AV})^2 + (x_2 - x_{AV})^2 + \cdots + (x_n - x_{AV})^2]} \tag{4.4}$$

Table 4.1: Tire deflections prepared by lab-view and obtained for passive experimental study.

Time(ms)	Tire Deflection (m)	Time(ms)	Tire Deflection (m)	Time(ms)	Tire Deflection (m)
19:24:34	0.03	**19:24:58**	-0.11	**19:25:22**	0.21
19:24:35	0.03	**19:24:59**	-0.14	**19:25:23**	0.14
19:24:36	0.07	**19:25:00**	0.06	**19:25:24**	0.12
19:24:37	0	**19:25:01**	0.14	**19:25:25**	0.03
19:24:38	-0.07	**19:25:02**	0.35	**19:25:26**	0.02
19:24:39	0.03	**19:25:03**	0.36	**19:25:27**	0.02
19:24:40	0.05	**19:25:04**	0.34	**19:25:28**	0.06
19:24:41	0.06	**19:25:05**	0.29	**19:25:29**	0.14
19:24:42	0.05	**19:25:06**	0.17	**19:25:30**	0.15
19:24:43	0.48	**19:25:07**	0.11	**19:25:31**	0.11
19:24:44	0.62	**19:25:08**	-0.09	**19:25:32**	0.1
19:24:45	0.6	**19:25:09**	-0.07	**19:25:33**	0.06
19:24:46	0.49	**19:25:10**	-0.02	**19:25:34**	0.04
19:24:47	0.03	**19:25:11**	0	**19:25:35**	0.04
19:24:48	-0.06	**19:25:12**	0.31	**19:25:36**	0.04
19:24:49	-0.14	**19:25:13**	0.31	**19:25:37**	0.04
19:24:50	-0.15	**19:25:14**	0.21	**19:25:38**	0.11
19:24:51	0.26	**19:25:15**	0.18	**19:25:39**	0.11
19:24:52	0.4	**19:25:16**	-0.01	**19:25:40**	0.1
19:24:53	0.48	**19:25:17**	-0.02	**19:25:41**	0.08
19:24:54	0.41	**19:25:18**	-0.02	**19:25:42**	0.08
19:24:55	0.39	**19:25:19**	-0.03	**19:25:43**	0.07
19:24:56	0.2	**19:25:20**	0.19	**19:25:44**	0.06
19:24:57	0	**19:25:21**	0.2	**19:25:22**	0.21

The numbers shown in table 4.1 presents the value of tire deflection for every one millisecond, and the average of this numbers is defined by RMS method. The average of deflection during passive work compare to stable deflection from suspension load was calculated as RMS number for stability evaluation. The number was defined (0.1515493 cm) and then it was compared with the same result in simulation. It used as (0.015155 m) and it multiplied with stiffness to define the tire load.

This calculation was repeated for other sets of data expression including tier and acceleration in active and passive in order to results reduction. And also for suspension travel, a calculation method used for the set of data in order to define suspension behaviours.

This method is using peak-to-peak of data's based on their amplitude and it is introduced with the abbreviation of "MPTP" [5]. It can be determined by comparison between minimum from maximum value of data and it's defined as:

$$\text{PTP (a)} = \text{maximum value of (a)} - \text{minimum value of (a)} \quad (4.5)$$

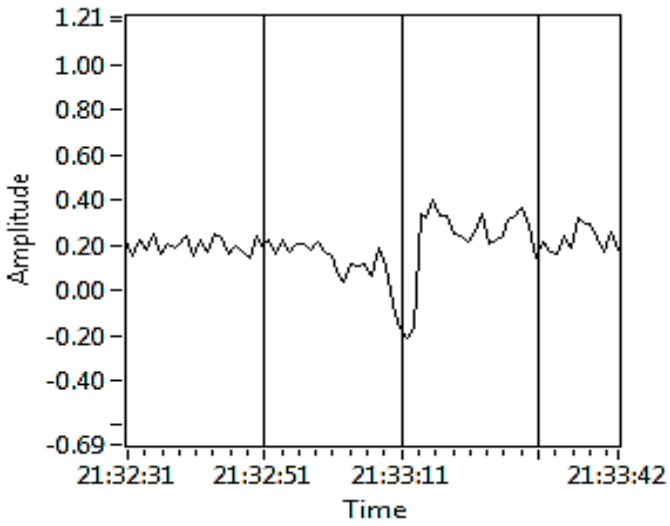

Figure 4.4: Diagram of suspension travel, amplitude (cm)-time(s), in active experimental test.

Table 4.2: Suspension travels were prepared by lab-view in active experimental study.

Time(ms)	Suspension Travel	Time(ms)	Suspension Travel	Time(ms)	Suspension Travel
21:32:32	0.16	**21:32:56**	0.21	**21:33:20**	0.24
21:32:33	0.22	**21:32:57**	0.21	**21:33:21**	0.22
21:32:34	0.18	**21:32:58**	0.18	**21:33:22**	0.26
21:32:35	0.25	**21:32:59**	0.22	**21:33:23**	0.34
21:32:36	0.16	**21:33:00**	0.17	**21:33:24**	0.21
21:32:37	0.21	**21:33:01**	0.15	**21:33:25**	0.23
21:32:38	0.19	**21:33:02**	0.06	**21:33:26**	0.25
21:32:39	0.21	**21:33:03**	0.04	**21:33:27**	0.31
21:32:40	0.24	**21:33:04**	0.12	**21:33:28**	0.33
21:32:41	0.15	**21:33:05**	0.11	**21:33:29**	**0.37**
21:32:42	0.22	**21:33:06**	0.12	**21:33:30**	0.29
21:32:43	0.17	**21:33:07**	0.06	**21:33:31**	0.14
21:32:44	0.25	**21:33:08**	0.18	**21:33:32**	0.21
21:32:45	0.23	**21:33:09**	0.11	**21:33:33**	0.17
21:32:46	0.16	**21:33:10**	-0.06	**21:33:34**	0.16
21:32:47	0.19	**21:33:11**	-0.16	**21:33:35**	0.24
21:32:48	0.17	**21:33:12**	**-0.22**	**21:33:36**	0.19
21:32:49	0.15	**21:33:13**	-0.17	**21:33:37**	0.32
21:32:50	0.24	**21:33:14**	0.34	**21:33:38**	0.3
21:32:51	0.19	**21:33:15**	0.32	**21:33:39**	0.29
21:32:52	0.23	**21:33:16**	0.4	**21:33:40**	0.23
21:32:53	0.16	**21:33:17**	0.33	**21:33:41**	0.17
21:32:54	0.23	**21:33:18**	0.33	**21:33:42**	0.26
21:32:55	0.17	**21:33:19**	0.25		

By taking pick to pick numbers, 0.37-(-0.22) =0.59 cm so, MPTP=0.059 m, and the method was repeated for active and passive, and also experimental and simulation study, in order to define MPTP for suspension travel. Validation evaluation requires specification of accuracy and inaccuracy for every segment separately in active and passive, based on simulation and experimental comparison. The equation (4.6) [5] shown below was used in order to define the percentage of inaccuracy for every part.

$$Inaccuracy(\%) = \left|\frac{Simulation(RMS) - Average\ of\ Experiments(RMS)}{Average\ of\ Experiment(RMS)} \times 100\right| \quad (4.6)$$

As a Final reduction a table was prepared including significant data's from suspension results, and it shown in table 4.3 below.

Table 4.3: Final results and inaccuracies defined in passive and active mode.

Passive Mode	**Units**	**Simulation**	**Experiment**	**Inaccuracy (%)**
Body Acceleration	RMS m/s^2	0.625	0.782	20.1
Dynamic Tire Force	RMS (N)	672.7	757.5	11.2
Suspension Travel	MPTP (m)	0.039	0.067	41.8
Active Mode	**Units**	**Simulation**	**Experiment**	**Inaccuracy (%)**
Body Acceleration	RMS m/s2	0.513	0.692	25.9
Dynamic Tire Force	RMS (N)	618.2	734.5	15.8
Suspension Travel	MPTP (m)	0.031	0.059	47.4

These results can show the accuracy of model in passive and active mode, and as it shown the accuracy in passive mode for simulation results is 75.7% and the accuracy in active mode is 70.3%, so it can shows a good conformity between simulation and experiment.

4.2 Ride Comfort Evaluation

Ride comfort was the essential approach in this study, and it's calculated from body acceleration. As the first criterion for performance improvement, the body acceleration was evaluated in active and passive mode. In this section, four acceleration results are presented for simulation and experimental in active and passive mode. The improvement result after this comparison is will be define in this part.

4.2.1 Simulation

The body acceleration was evaluated in active and passive mode during MATLAB-Simulink simulation and the comparison was based on RMP number. Both of results are shown in one diagram below in fig.4.5.

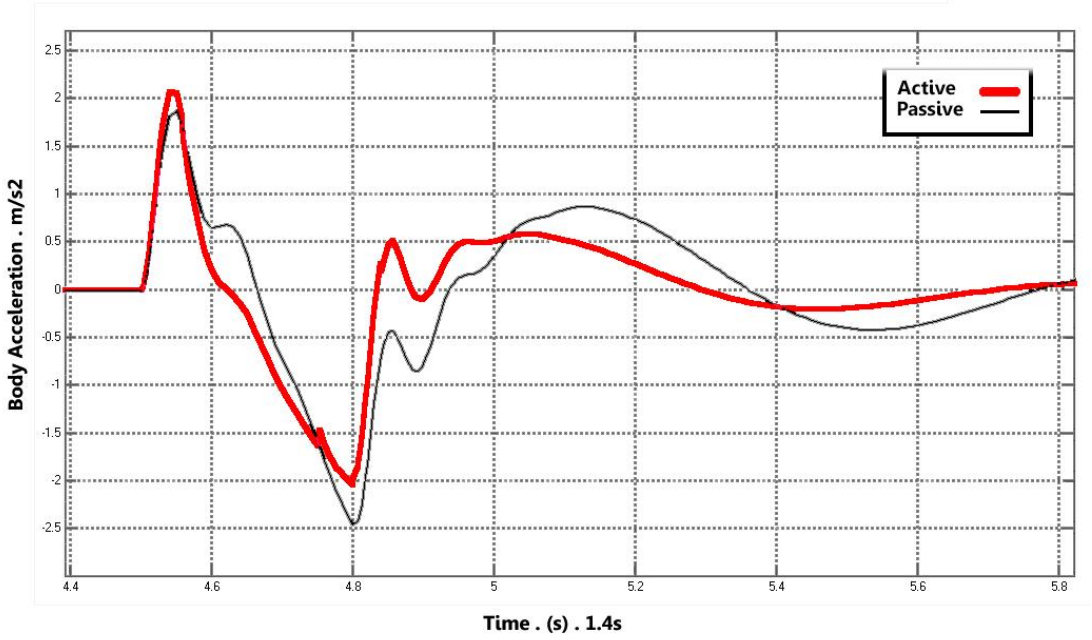

Figure 4.5: Simulink Diagram for body acceleration in active and passive mode during 1400ms simulation test.

The RMS values for active and passive mode were defined, (0.513 m/s^2) and (0.625 m/s^2) respectively. With a simple calculation using equation (4.7) [5] below, the percentage of comfort improvement in simulation was defined.

$$improvement\ (\%) = \left|\frac{(active\ RMS)-(passive\ RMS)}{passive\ RMS}\right| \times 100 \qquad (4.7)$$

4.2.2 Experimental

Ride comfort was also evaluated experimentally by using RMS values were defined in model validation part mentioned before and equation 4.7 used to define percentage of experimentally improvement during a limited time. The fig.4.6 below shows diagram of acceleration in 2160ms of experimental study in passive mode.

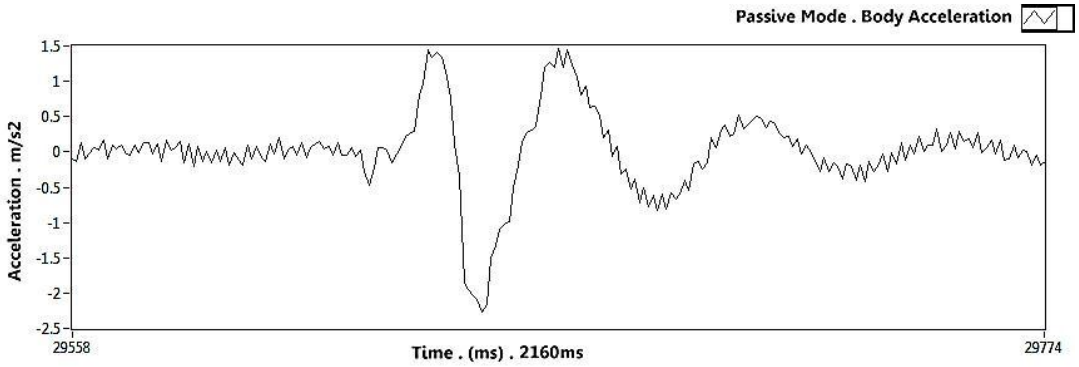

Figure 4.6: Diagram for body acceleration in passive mode during 2160ms simulation test.

The details of this diagram are presented in table 4.4 below. This detail shown was used to define RMS value of diagram and then the result of passive acceleration will be comparison with body acceleration in active mode.

Table 4.4: Body acceleration results obtained from passive experimental study.

Time(ms)	Acceleration m/s^2	Time(ms)	Acceleration m/s	Time(ms)	Acceleration m/s
4807	-0.0112721	4850	1.18971	4893	0.0158916
4808	0.0319079	4851	1.20338	4894	-0.0334612
4809	0.0274508	4852	1.08626	4895	-0.0450251
4810	-0.00896144	4853	0.655074	4896	0.00919833
4811	-0.00964808	4854	0.556362	4897	-0.00581817
4812	-0.00998536	4855	0.589263	4898	-0.0190867
4813	-0.0310944	4856	0.53863	4899	-0.0304121
4814	0.00363879	4857	0.551814	4900	-0.00803517
4815	0.00297696	4858	0.421357	4901	-0.0194194
4816	0.00229994	4859	0.166098	4902	-0.00795696
4817	0.0121756	4860	-0.130263	4903	-0.0396584
4818	-0.0109746	4861	-0.296732	4904	0.0174807
4819	0.0319038	4862	-0.352759	4905	-0.0162603
4820	0.0693648	4863	-0.0974225	4906	-0.00380273
4821	0.543877	4864	-0.129735	4907	-0.0136399
4822	0.678767	4865	-0.102138	4908	-0.00096007
4823	0.969955	4866	-0.222109	4909	-0.0317738
4824	0.928653	4867	-0.544544	4910	0.0153861
4825	0.981251	4868	-0.553804	4911	0.0149607
4826	0.821089	4869	-0.430212	4912	-0.00694227
4827	0.770446	4870	-0.328387	4913	-0.00525186
4828	0.597795	4871	-0.217321	4914	0.0175037
4829	0.384195	4872	-0.153901	4915	0.0268196
4830	0.0767859	4873	-0.0505617	4916	-0.00779779

The body acceleration in passive mode was compared with active suspension results in experimental test. This test and its results are shown in fig.4.7 and table 4.5 below. And also the complete results for body acceleration in passive and active experimental test are available in appendix, tables A-1 and A-2.

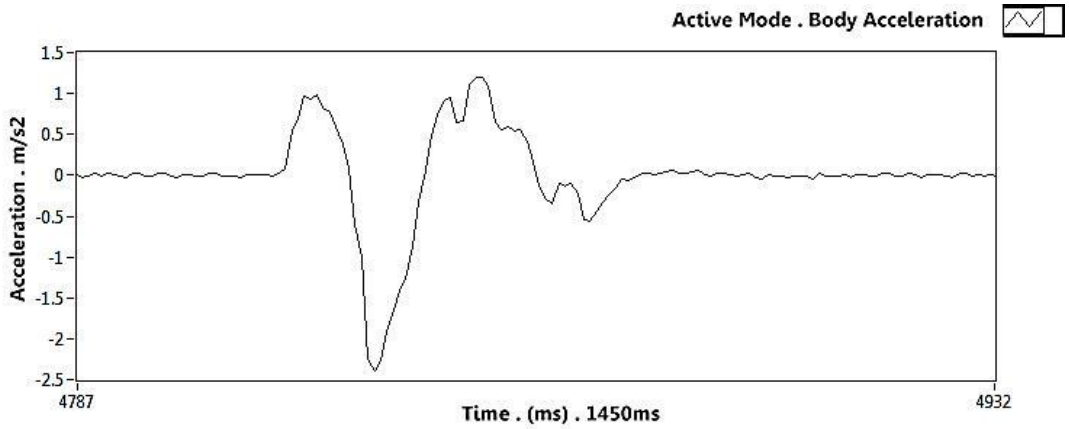

Figure 4.7: Diagram for body acceleration in active mode during 1450ms simulation test.

Table 4.5: Body accelerations were prepared by lab-view in active experimental study.

Time(ms)	Acceleration m/s^2	Time(ms)	Acceleration m/s	Time(ms)	Acceleration m/s
29580	0.016164	**29623**	-0.282991	**29666**	1.47328
29581	0.0589766	**29624**	-0.470744	**29667**	1.20209
29582	0.15214	**29625**	-0.228508	**29668**	1.45181
29583	-0.151944	**29626**	0.0525402	**29669**	1.23951
29584	0.106942	**29627**	0.0571482	**29670**	1.04959
29585	-0.204157	**29628**	0.0274897	**29671**	0.802718
29586	0.0696437	**29629**	-0.14941	**29672**	0.93896
29587	-0.141928	**29630**	-0.0208869	**29673**	0.628872
29588	0.0152431	**29631**	0.0617215	**29674**	0.643559
29589	-0.160077	**29632**	0.223732	**29675**	0.518503
29590	0.0327987	**29633**	0.247738	**29676**	0.207835
29591	-0.140323	**29634**	0.296359	**29677**	0.305979
29592	0.0540806	**29635**	0.811097	**29678**	-0.0583171
29593	-0.19189	**29636**	0.971845	**29679**	0.0776033
29594	-0.0137073	**29637**	1.45114	**29680**	-0.31906
29595	-0.115302	**29638**	1.33116	**29681**	-0.240391
29596	-0.190071	**29639**	1.4061	**29682**	-0.526885
29597	0.101118	**29640**	1.33174	**29683**	-0.379693
29598	-0.0952966	**29641**	1.13587	**29684**	-0.724271
29599	0.0858353	**29642**	0.764709	**29685**	-0.502426
29600	-0.089163	**29643**	0.117597	**29686**	-0.7829
29601	-0.140223	**29644**	-0.347605	**29687**	-0.614469

The equation (4.7) were used to define percentage of comfort improvement Calculate percentage of comfort improvement and the final results for comfort improvement in simulation and experimental are shown in table 4.6 below.

Table 4.6: Simulate and experiment RMS results of body accelerations for active and passive suspension.

Mode	**Passive (RMS) m/s^2**	**Active (RMS) m/s^2**	**Improvement (%)**
Simulation	0.625	0.513	17.92
Experimental	0.782	0.692	11.51

As it shows the simulation result has better improvement in comfort, and the control model achieved to get (11.51%) experimentally improvement.

4.3 Stability Evaluation

The handling capability of active suspension was evaluated after comfort. As it was mentioned before, a passive suspension is in a compromise between comfort and handling, if the new suspension has performance improvement in comfort, by decreasing performance in handling, it will automatically disqualify significant improvement from control strategy.

4.3.1 Simulation

The tire deflection and then tire load was investigated in order to define stability in simulation. These tire loads in active and passive mode both are shown fig.4.8

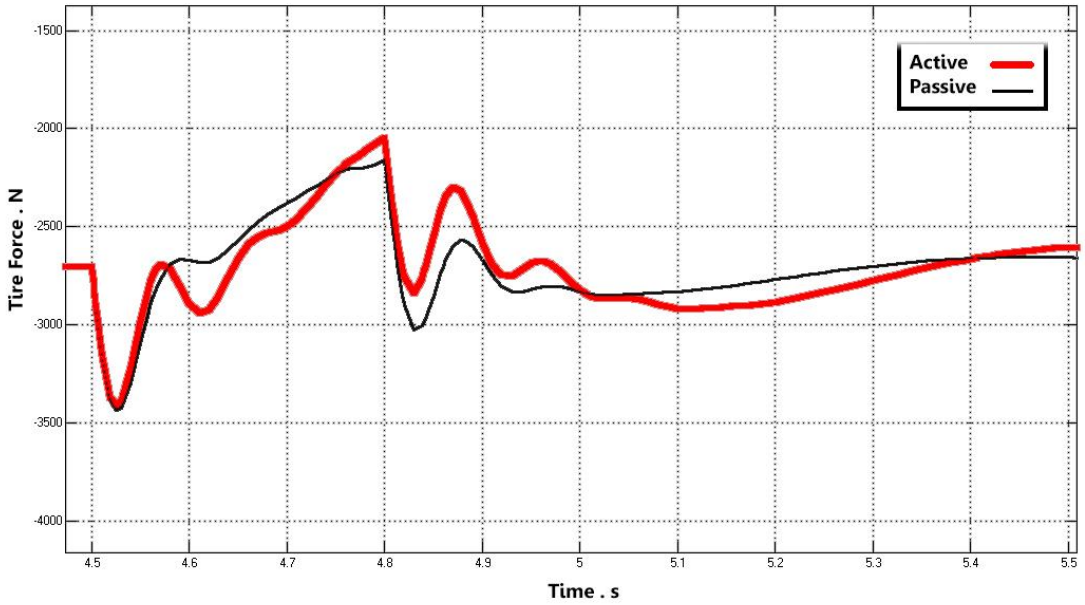

Figure 4.8: Diagram of tire force in passive and active simulation test.

4.3.2 Experimental

As it mentioned before, forces are applying to tire have significant role in suability evaluation. In experimental part, the tire force was defined from tire deflection in order to investigate the stability. Diagrams of experimentally tire deflection for passive and active test are shown in fig.4.9 and fig.4.10 respectively. And also the complete test details for tire forces are available in appendix, tables A-3 and A-4.

.

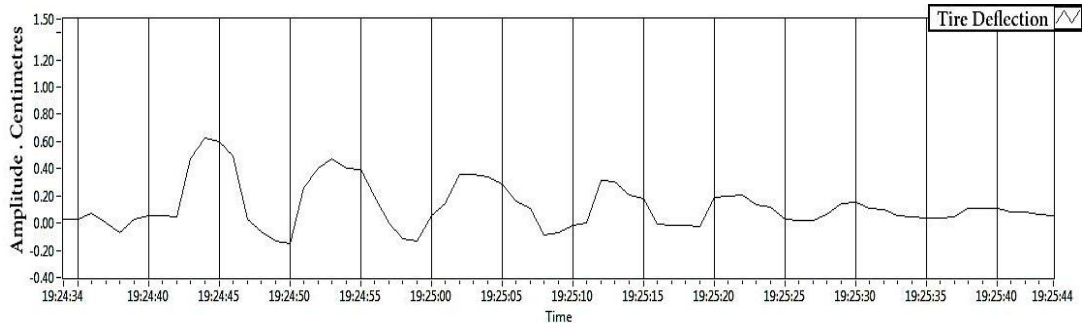

Figure 4.9: Diagram of tire deflection in passive experimental test.

After experimental passive test, the model was tested in active mod with same excitation to investigate tire deflection between active and passive.

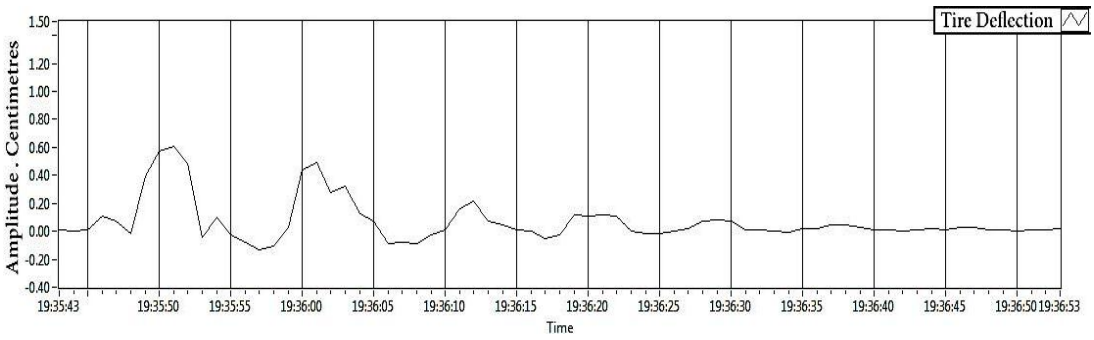

Figure 4.10: Diagram of tire deflection in active experimental test.

The RMS values for both of these active and passive tests were specified by using equation (4.2) as a reductive function in order to defied stability performance.

Simulation and experimental results in active and passive tests for tire forces are specified, and also their performances are separately evaluated by equation (4.7) and shown in table 4.7 below.

Table 4.7: Simulate and experiment RMS results of tire forces for active and passive suspension.

Mode	Passive (RMS) N	Active (RMS) N	Improvement (%)
Simulation	672.7	618.2	8.1
Experimental	757.5	734.5	3.04

The result shows handling performance of new suspension didn't reduce but also it (8.1%) simulative and (3.04%) experimentally improved.

4.4 Suspension Travel

After dynamic factors, another important investigation for suspension performance is structural improvement. More suspension travel requires more strokes which has negative effect on vehicle stability, specifically in speed race cars. The MPTP value from suspension travel used as a reductive function was evaluated to define pick to pick suspension travel as a structural performance. And it was investigated in simulation and experimentally.

4.4.1 Simulation

Suspension travel was simulated in Simulink is shown in fig.4.11 and fig.4.12 for active and passive modes.

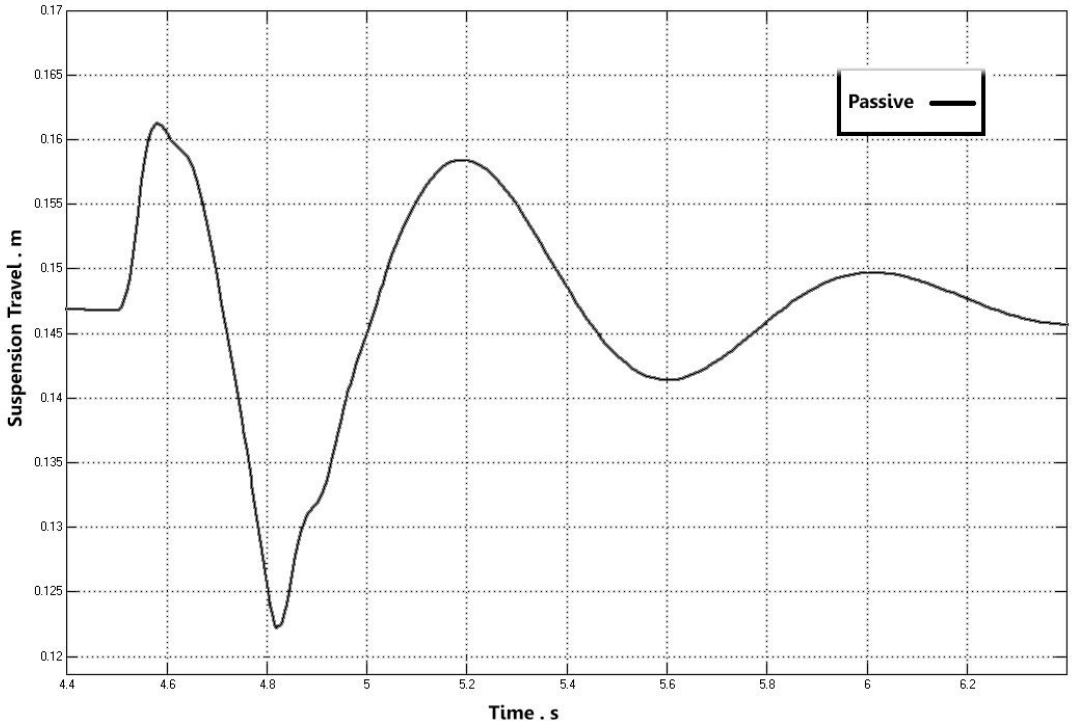

Figure 4.11: Suspension travel in passive simulation test.

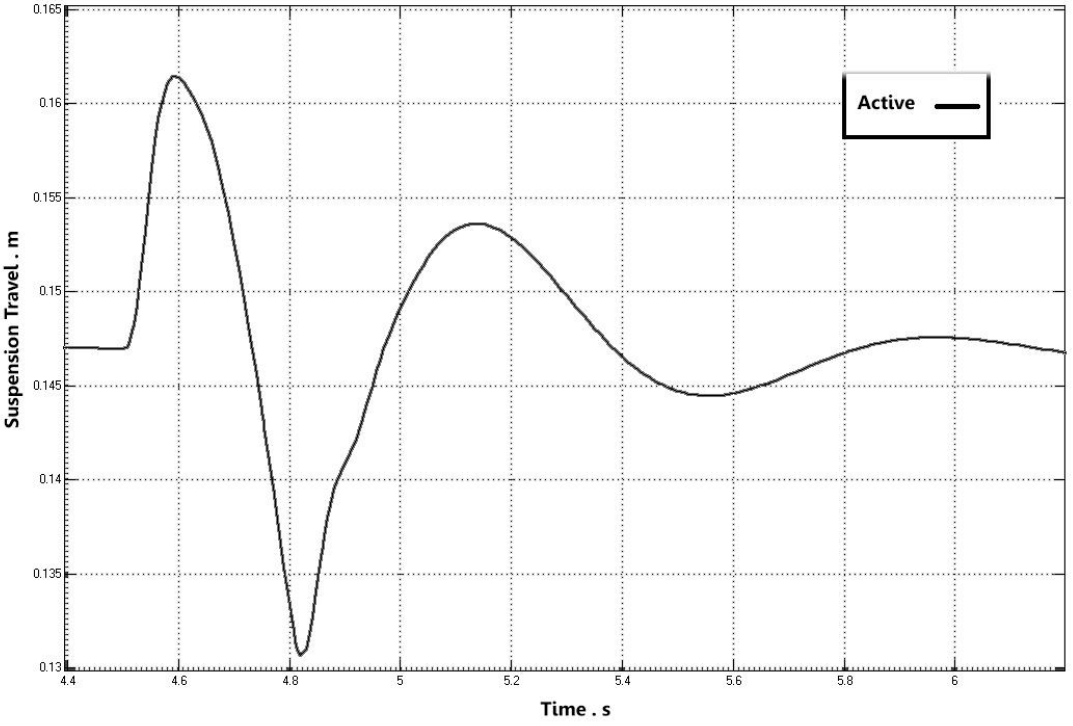

Figure 4.12: Suspension travel in active simulation test.

4.4.2 Experimental

The suspension travel was defined experimentally in active and passive study, in order to evaluate structural performance experimentally. Results are shown in fig.4.13 and fig.4.14 from passive and active tests respectively. More details and table of results are available in appendix A, tables A-5 and A-6.

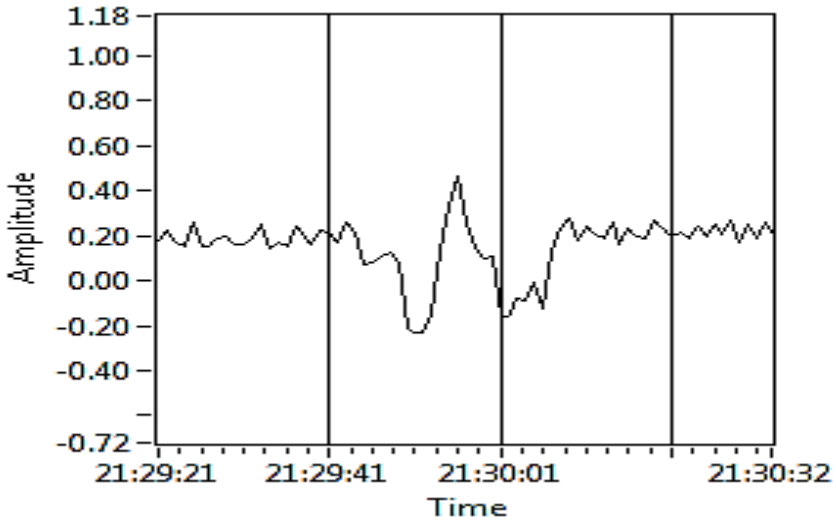

Figure 4.13: Suspension travel (decimetre) in passive experimental test.

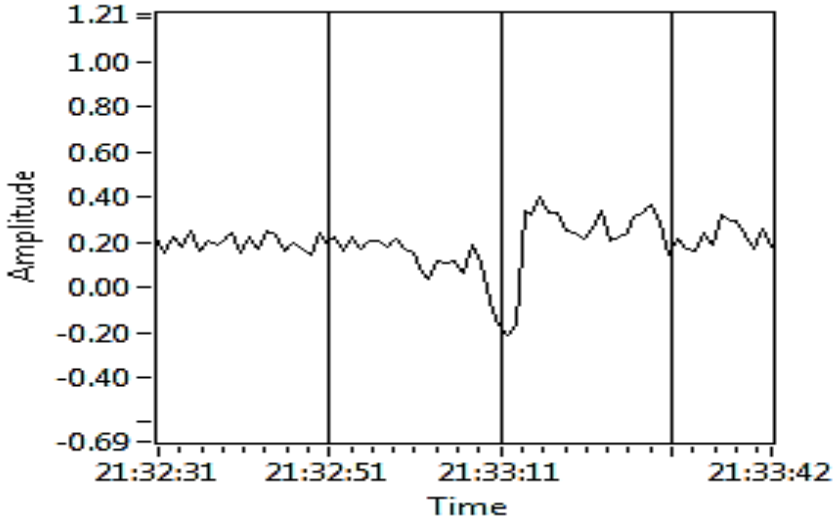

Figure 4.14: Suspension travel (decimetre) in active experimental test.

The MPTP value of Suspension travel results from simulate and experiment was used to evaluate percentage of improvement, experimentally or in simulative. And results are shown in table 4.8 below.

Table 4.8: Simulation and experimental based RMS results of suspension travel for active and passive modes.

Mode	**Passive (MPTP) m**	**Active (MPTP) m**	**Improvement (%)**
Simulation	0.0396	0.0317	19.95
Experimental	0.067	0.059	11.94

The results table shows the suspension travel had structural improved. It had (19.95%) simulative and (11.94%) experimentally improvement to lower required stroke. And it means the new suspension can vibrate in less suspension displacement.

Fig.4.15, fig.4.16 and fig.4.17 are shown below present charts for suspension comfort, handling and suspension travel, simulative and experimentally. And finally the percentage of suspension improvement and the simulation validity are shown in fig.4.18

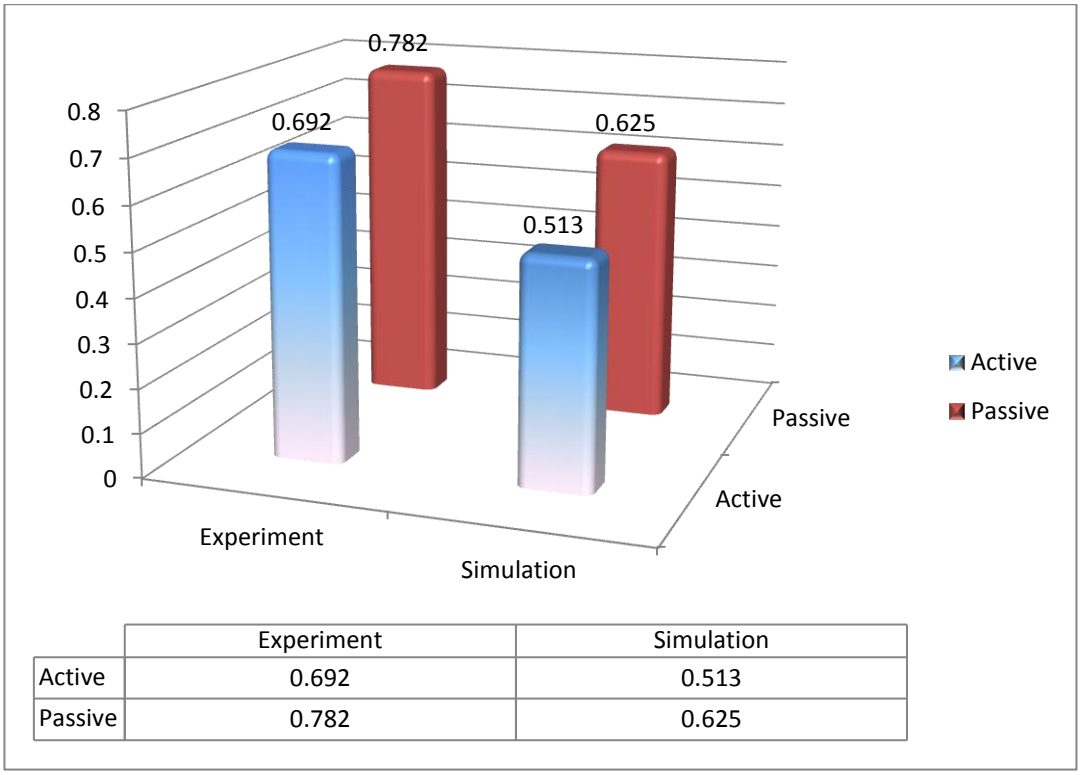

	Experiment	Simulation
Active	0.692	0.513
Passive	0.782	0.625

Figure 4.15: Chart of comfort in passive and active, simulation and experiment test.

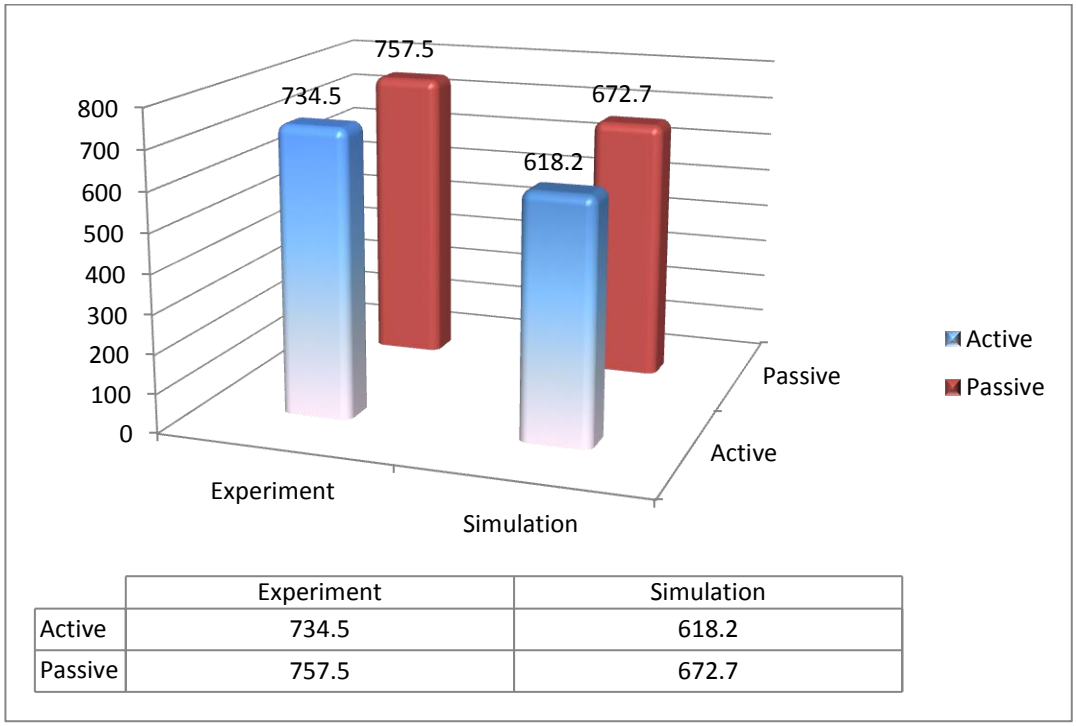

	Experiment	Simulation
Active	734.5	618.2
Passive	757.5	672.7

Figure 4.16: Chart of dynamic force in passive and active, simulation and experiment test.

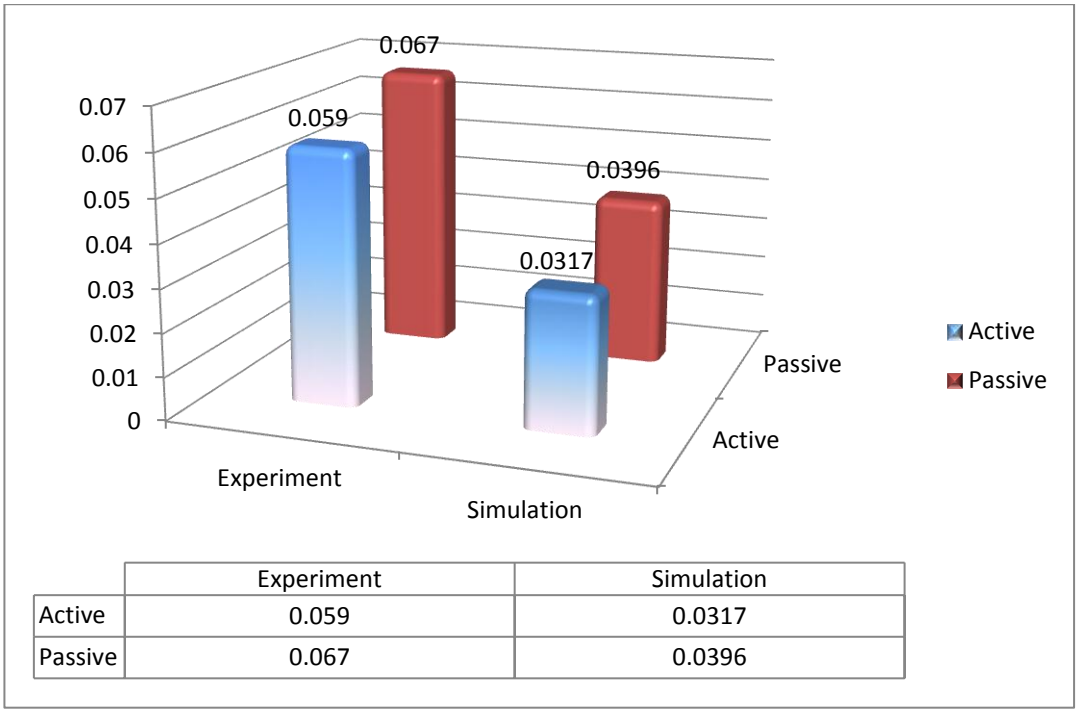

	Experiment	Simulation
Active	0.059	0.0317
Passive	0.067	0.0396

Figure 4.17: Chart of suspension travel in passive and active, simulation and experiment test.

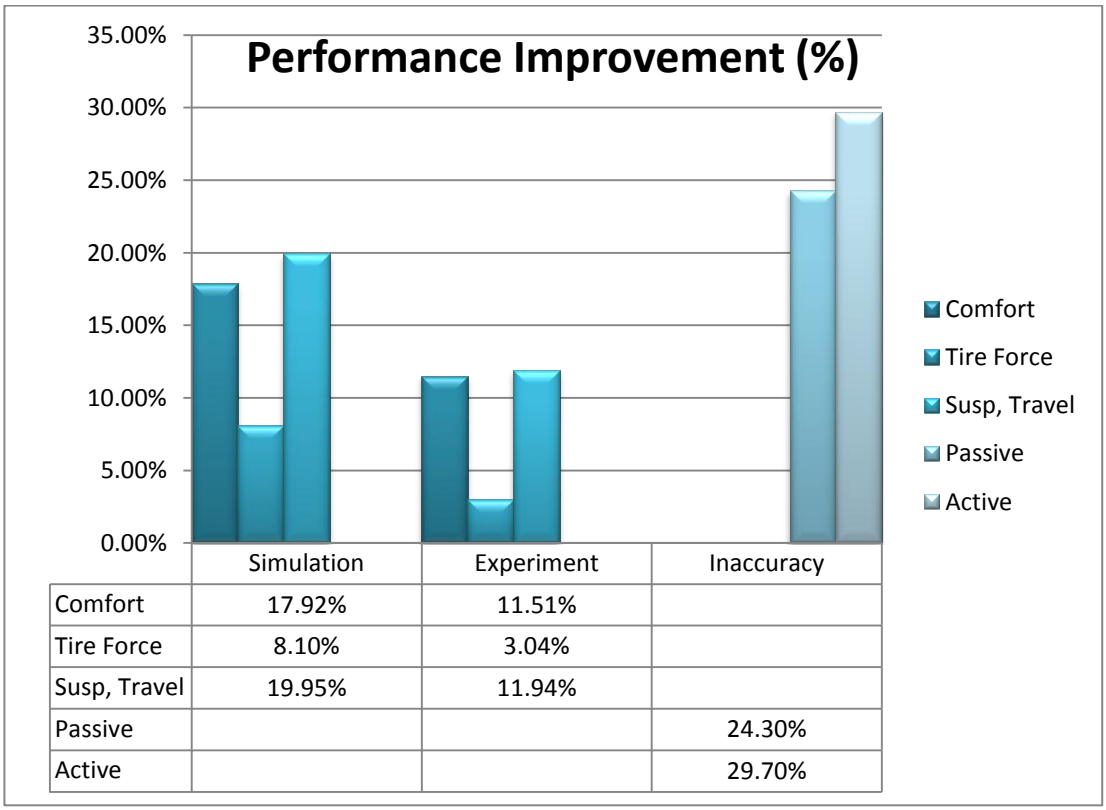

	Simulation	Experiment	Inaccuracy
Comfort	17.92%	11.51%	
Tire Force	8.10%	3.04%	
Susp, Travel	19.95%	11.94%	
Passive			24.30%
Active			29.70%

Figure 4.18: Chart of final performance improvement.

Chapter 5

CONCLUSION

5.1 Summary and Conclusions

In this section, the work will be summarized including other studies related to this study as well. The objectives of this research was improving comfort performance of suspension for pneumatic vibration isolation specifically passenger cars and vehicles which are more dependent on pneumatic suspensions. In order to achieve this approach, a quarter of a passenger car was simulative and experimentally modelled. The quarter-car suspension was a model of air suspension with a weak shock-absorber in order to have more focus on pneumatic vibration isolation. The air spring was collected from track cabin suspension and the shock-absorber was belongs to a small passenger car. The reason for selecting a passenger car as model was discussion about a complete control strategy for suspension comfort, stability and stork place in order to improve real performance in suspension system.

Before starting this study, a normal quarter-car suspension was modelled in MATLAB-Simulink for suspension performance evaluation and its improvement investigation in parameters variations. The idea of stiffness based suspension optimization was simulate and tested in order to investigate the possibility of control, based on stiffness variation. Then a simulation and experimental model was prepared at the same time and with same features for validity evaluation at the end of study.

Modelling of new suspension was consisted of three parts, modelling of sensors whish was specifying relation between resistance or voltage, and displacement or pressure in computer. Modelling of actuators which were calculating the relation between binary orders and force in suspension. Modelling of controller, which was calculating correct activation order from suspension equation.

Two of position sensors were installed directly between road and wheel, and other one installed between body and wheel, in order to get better accuracy from simulation. And one position sensor was installed to sense the road. a test was designed and prepared to evaluate the performance of suspension. Road simulator was simulating speed hump and lab-view was receiving this data with a sensor was installed in road simulator. Controller was charge and discharging the air spring in order to increase suspension dynamic and structural performance.

Results of simulation and experimental was evaluated separately, to define the comfort, stability and suspension travel performance. And also the validity of simulation was defined by comparison between simulation and experimental MPTP and RMS values. The percentage of inaccuracy was the reason for non-conformity, as it shows in fig.5.1 below.

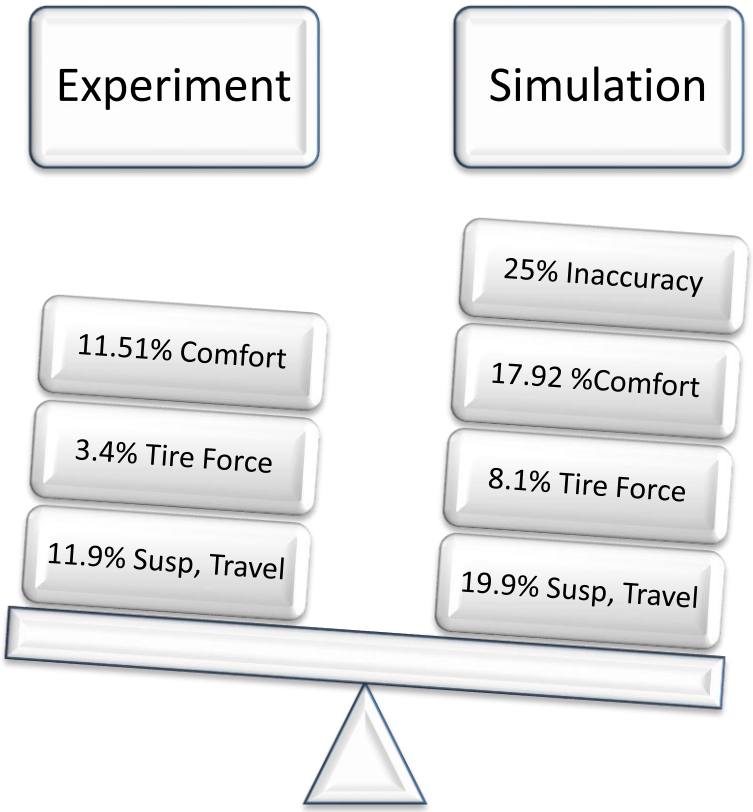

Figure 5.1: Chart for inaccuracy of simulation.

After suspension examination, the acceleration of body was defined. The body acceleration was 17.92% improved in simulation and 11.51% experimentally. This shows a significant improvement for ride comfort. The suspension also examined in order to define handling performance in simulation and experiment, handling performance was defined from tire force and it improved 8.1% simulative and 3.04% experimentally. The structural improvement also was defied from suspension travel and it also improved 19.95% in simulation and 11.94% experimentally. Considering this improvement has an essential role to decrease the suspension stroke.

5.2 Future Work

As it was mentioned before in this study, air-suspension had become prevalent in different vehicle todays, and software based reformation an economized solution in order to optimize suspension performance. The control strategy used during this study was mathematical based, which tries to improve performance, by simulating suspension and its actuators. However mathematical simulation can never have 100% validity or accuracy compare to an experimental test.

These types of control methods are strongly dependent on predictive equations for undesired variations prevention. In other side the new controller wants to be adjustable to control every suspension due to suspension specifications. So the other difficulty is to define and introduce the complete and correct details from suspension to the controller. And it will not finish up to here, because the mathematical based controller requires lots of sensors and it has heavy calculation.

For example for actuators simulation, all of part was modeled from electric solenoid, throttle, dynamic and static capacity of chamber and pipes, air flow to pressure conversion, pressure to force conversion, to finally static and dynamic friction. All these process was done in order to define force from binary order. However if the controller follow a table of information between force and binary order, it can even more validation compare to simulation. But the question is how this table can be prepared with the adjustability was mentioned before? The only capability the new controller need, it the ability of learning. This method called genetic algorithm

It learn by itself, it prepare a list of information in a neural network based on experiment, so there is no simulation or in other word the simulation validity is 100%. Also this method experimentally has better control on time delay.

REFERENCES

[1] Winfred K. N. Anakwa, Dion R. Thomas, Scott C. Jones, Jon Bush, Dale Green, George W. Anglin, Ron Rio, Jixiang Sheng, Scott Garrett, and Li Chen, "Development and Control of a Prototype Pneumatic Active Suspension System" *Education, IEEE Transactions*, 2002, Vol. 45, No. 1, pp. 43-49.

[2] Chandramouli Padmanabhan, "Semi-active hydro-gas suspension system for a tracked vehicle", *Journal of Terramechanics*, 2011, vol.48, No. 3, pp. 225–239.

[3] Yun-Ho Shin, Kwang-Joon Kim, "Performance enhancement of pneumatic vibration isolation tables in low frequency range by time delay control", *Journal of Sound and Vibration*, 10 April 2009, 537–553.

[4] Colin Gordon, "Generic vibration criteria for vibration- sensitive equipment", *Optomechanical Engineering and Vibration Control*, 28 September 1999, 22-33.

[5] Shahriar Sarami, "Development and Evaluation of a Semi-active Suspension System for Full Suspension Tractors", *Thesis presented to Technische University Berlin*, 2 September 2009, http://opus.kobv.de/tuberlin/volltexte/2010/2499/

[6] Nima Eslaminasab, "Development of a Semi-active Intelligent Suspension System for Heavy Vehicles", *Thesis presented to University of Waterloo*, 2008, http://hdl.handle.net/10012/3658.

[7] Bjorn O. Svartz Jamestown, Darris White, Superior, "Electronic Height control", *United States Patent*, 2005, Patent No. US 6,959,932 B2.

[8] Whiteknight, "Control Systems and control engineering", *Wikibooks*, 2007, http://en.wikibooks.org/wiki/Control_Systems/Transfer_Functions.

[9] Dr. Gleb, V. Tcheslavski, "Optimum filters" ELEN 5301 Adv, *DSP and Modeling, Lecture* 06, 2008, page. 27. http://www.ee.lamar.edu/ gleb/adsp/Index.htm.

[10] Hans-Peter Schöner, "Automotive mechatronics" *Control Engineering Practice*, (2004), vol. 12, No. 11, pp. 1343-1351.

[11] Emir Sakman, Rahmi Guclu, Nurkan Yagiz, "Fuzzy logic control of vehicle suspensions with dry friction nonlinearity", *Sadhana*, October 2005, Vol. 30, Issue 5, pp. 649-659.

[12] Lallart, Mickael. "Vibration Control." *Hard cover, Publisher InTech*, (2010).

[13] Chassis Tech Wholesale "Popular Air suspension Solutions", Accessed on 16th of May 2012, http://www.airbagit.com/Air-Shocks-s/30.htm.

[14] Mike Hanlon "Bose Redefines Automobile Suspension Systems", *gizmag*, Accessed on 11th of July 2012, http://www.gizmag.com/go/3259/

[15] Hendrickson trailer air ride suspension schematic, *lulusoso*, Accessed on 25th of July 2012, http://www.lulusoso.com/products/Hendrickson-Trailer-Air-Ride-Suspension-Schematic.html

[16] Van den Brink, "Modelling and control of a robotic arm actuated by nonlinear artificial muscles", *Technische Universiteit Eindhoven*, 2007, XI.174 p.

[17] Zhihong Yin, Amir Khajepour, Dongpu Cao, Babak Ebrahimi & Konghui Guo, "A new pneumatic suspension system with independent stiffness and ride height tuning

capabilities", *International Journal of Vehicle Mechanics and Mobility,* 24 Feb 2012, pages 1-164.

[18] Digikey, "Flex Sensor", *Spectra Symbol,* 2012, http://www.digikey.com/us/en/ph/SpectraSymbol/flex_sensor.html

[19] Serdar Yildirim, "Vibration control of suspension systems using a proposed neural network", *Journal of Sound and Vibration,* (2004), Vol.277.Issues 4–5, 1059–1069.

[20] Rainswang "5/3 Solenoid Valve/ Double Power 4V230C-08", *made in china* http://rainswang.en.made-in-china.com/product/zegEpPmAONks/China-5-3-Solenoid-Valve-Double-Power-4V230C-08-.html

[21] Aircraft, "206001K", Mercedes, Actros. 1831.1860. Rear, Accessed on 4th of December 2012, http://www.airkraft.com.tr/sayfalar.asp?pageID=Urunler&tipi=8

APPENDICES

Appendix A: Results

Table A-1: Experimental results, passive, body acceleration

Time(ms)	Acceleration m/s^2	Time(ms)	Acceleration m/s	Time(ms)	Acceleration m/s
4788	-0.0213831	4826	0.821089	4864	-0.129735
4789	-0.0185313	4827	0.770446	4865	-0.102138
4790	0.0161901	4828	0.597795	4866	-0.222109
4791	-0.00593589	4829	0.384195	4867	-0.544544
4792	0.0166201	4830	0.0767859	4868	-0.553804
4793	0.015236	4831	-0.590547	4869	-0.430212
4794	-0.0180787	4832	-1.01248	4870	-0.328387
4795	-0.0262817	4833	-2.25744	4871	-0.217321
4796	0.019862	4834	-2.38936	4872	-0.153901
4797	0.0289467	4835	-2.27033	4873	-0.0505617
4798	-0.0059383	4836	-1.90911	4874	-0.0621117
4799	-0.00534631	4837	-1.64739	4875	-0.0284904
4800	0.0164299	4838	-1.40841	4876	0.0234986
4801	0.0249011	4839	-1.2705	4877	0.0271579
4802	-0.0104164	4840	-0.868403	4878	-0.00198993
4803	-0.0206296	4841	-0.336337	4879	0.0247117
4804	0.0130082	4842	0.0647863	4880	0.0478957
4805	0.0110985	4843	0.48492	4881	0.0567234
4806	-0.0120207	4844	0.741319	4882	0.0313591
4807	-0.0112721	4845	0.917711	4883	0.0288572
4808	0.0319079	4846	0.954207	4884	0.046887
4809	0.0274508	4847	0.643012	4885	0.0616827
4810	-0.00896144	4848	0.672943	4886	-0.00066528
4811	-0.00964808	4849	1.11278	4887	-0.00370365
4812	-0.00998536	4850	1.18971	4888	0.0253268
4813	-0.0310944	4851	1.20338	4889	0.029492
4814	0.00363879	4852	1.08626	4890	0.0112869
4815	0.00297696	4853	0.655074	4891	-0.00532246
4816	0.00229994	4854	0.556362	4892	0.0116114
4817	0.0121756	4855	0.589263	4893	0.0158916
4818	-0.0109746	4856	0.53863	4894	-0.0334612
4819	0.0319038	4857	0.551814	4895	-0.0450251
4820	0.0693648	4858	0.421357	4896	0.00919833
4821	0.543877	4859	0.166098	4897	-0.00581817
4822	0.678767	4860	-0.130263	4898	-0.0190867
4823	0.969955	4861	-0.296732	4899	-0.0304121
4824	0.928653	4862	-0.352759	4900	-0.00803517
4825	0.981251	4863	-0.0974225	4901	-0.0194194

Table A-1: Experimental results for passive, body acceleration (Continued)

Time(ms)	Acceleration m/s^2	Time(ms)	Acceleration m/s	Time(ms)	Acceleration m/s
4902	-0.00795696	4912	-0.00694227	4922	0.0146871
4903	-0.0396584	4913	-0.00525186	4923	0.0128758
4904	0.0174807	4914	0.0175037	4924	-0.0102064
4905	-0.0162603	4915	0.0268196	4925	-0.0200235
4906	-0.00380273	4916	-0.00779779	4926	0.0244979
4907	-0.0136399	4917	-0.0174601	4927	0.0214524
4908	-0.00096007	4918	0.0271262	4928	-0.0135259
4909	-0.0317738	4919	0.0135165	4929	0.00829402
4910	0.0153861	4920	-0.0306892	4930	-0.00405627
4911	0.0149607	4921	0.00445662	4931	0.00610204

Table A-2: Experimental results for active, body acceleration

Time(ms)	Acceleration m/s^2	Time(ms)	Acceleration m/s	Time(ms)	Acceleration m/s
29559	-0.139608	**29602**	0.12024	**29645**	-1.8499
29560	0.127231	**29603**	-0.0323949	**29646**	-1.95503
29561	-0.103805	**29604**	0.210688	**29647**	-2.03868
29562	-0.0189661	**29605**	-0.108007	**29648**	-2.09467
29563	0.0533645	**29606**	0.029822	**29649**	-2.26042
29564	0.0265636	**29607**	0.0785858	**29650**	-2.16973
29565	0.158093	**29608**	-0.045453	**29651**	-1.50702
29566	-0.0984544	**29609**	0.131314	**29652**	-1.3327
29567	0.0888245	**29610**	-0.0807321	**29653**	-1.09651
29568	0.0359906	**29611**	0.0538921	**29654**	-1.02569
29569	0.0891671	**29612**	0.109191	**29655**	-0.989083
29570	-0.0302148	**29613**	0.148964	**29656**	-0.500375
29571	-0.0391169	**29614**	0.0465998	**29657**	-0.188477
29572	0.101306	**29615**	0.0840511	**29658**	0.145108
29573	-0.0188884	**29616**	-0.0395613	**29659**	0.271364
29574	0.129028	**29617**	0.127054	**29660**	0.311413
29575	0.131826	**29618**	-0.052459	**29661**	0.363446
29576	-0.0271322	**29619**	-0.0453128	**29662**	0.795449
29577	0.10528	**29620**	0.0687143	**29663**	1.19327
29578	-0.127608	**29621**	-0.0656558	**29664**	1.26324
29579	0.167487	**29622**	0.0170221	**29665**	1.19568
29580	0.016164	**29623**	-0.282991	**29666**	1.47328
29581	0.0589766	**29624**	-0.470744	**29667**	1.20209
29582	0.15214	**29625**	-0.228508	**29668**	1.45181
29583	-0.151944	**29626**	0.0525402	**29669**	1.23951
29584	0.106942	**29627**	0.0571482	**29670**	1.04959
29585	-0.204157	**29628**	0.0274897	**29671**	0.802718
29586	0.0696437	**29629**	-0.14941	**29672**	0.93896
29587	-0.141928	**29630**	-0.0208869	**29673**	0.628872
29588	0.0152431	**29631**	0.0617215	**29674**	0.643559
29589	-0.160077	**29632**	0.223732	**29675**	0.518503
29590	0.0327987	**29633**	0.247738	**29676**	0.207835
29591	-0.140323	**29634**	0.296359	**29677**	0.305979
29592	0.0540806	**29635**	0.811097	**29678**	-0.0583171
29593	-0.19189	**29636**	0.971845	**29679**	0.0776033
29594	-0.0137073	**29637**	1.45114	**29680**	-0.31906
29595	-0.115302	**29638**	1.33116	**29681**	-0.240391
29596	-0.190071	**29639**	1.4061	**29682**	-0.526885
29597	0.101118	**29640**	1.33174	**29683**	-0.379693
29598	-0.0952966	**29641**	1.13587	**29684**	-0.724271
29599	0.0858353	**29642**	0.764709	**29685**	-0.502426
29600	-0.089163	**29643**	0.117597	**29686**	-0.7829
29601	-0.140223	**29644**	-0.347605	**29687**	-0.614469

Table A-2: Experimental results for active, body acceleration (Continued)

Time(ms)	Acceleration m/s^2	Time(ms)	Acceleration m/s	Time(ms)	Acceleration m/s
29688	-0.828185	29717	0.225968	**29746**	0.228702
29689	-0.604952	**29718**	0.0753749	**29747**	0.0140707
29690	-0.819198	**29719**	0.192535	**29748**	0.101604
29691	-0.586406	**29720**	-0.0358186	**29749**	0.0894329
29692	-0.665353	**29721**	0.0929866	**29750**	0.318036
29693	-0.590623	**29722**	-0.0162401	**29751**	0.0141925
29694	-0.400218	**29723**	-0.121363	**29752**	0.100383
29695	-0.546233	**29724**	-0.272113	**29753**	0.266635
29696	-0.179958	**29725**	-0.0837263	**29754**	0.0407722
29697	-0.129175	**29726**	-0.279711	**29755**	0.296562
29698	-0.237293	**29727**	-0.156949	**29756**	0.146763
29699	-0.157251	**29728**	-0.213984	**29757**	0.188355
29700	0.197679	**29729**	-0.391178	**29758**	0.0665988
29701	0.0597265	**29730**	-0.162641	**29759**	0.274877
29702	0.303843	**29731**	-0.202223	**29760**	-0.00489278
29703	0.374154	**29732**	-0.405526	**29761**	0.0628329
29704	0.221612	**29733**	-0.191366	**29762**	0.159352
29705	0.25945	**29734**	-0.423368	**29763**	-0.0362247
29706	0.522733	**29735**	-0.13187	**29764**	0.166311
29707	0.331968	**29736**	-0.269643	**29765**	-0.116328
29708	0.382692	**29737**	-0.165407	**29766**	-0.101619
29709	0.455434	**29738**	-0.0294655	**29767**	0.0951668
29710	0.504736	**29739**	-0.278199	**29768**	-0.0867278
29711	0.466997	**29740**	-0.00575496	**29769**	0.0242024
29712	0.335907	**29741**	-0.16454	**29770**	0.0150548
29713	0.434666	**29742**	0.128206	**29771**	-0.194854
29714	0.39417	**29743**	-0.109291	**29772**	-0.0549814
29715	0.272455	**29744**	0.0958818	**29773**	-0.192601
29716	0.202347	**29745**	-0.0244349		

Table A-3: Experimental results for passive, tire deflection

Time(ms)	Tire Deflection (m)	Time(ms)	Tire Deflection (m)	Time(ms)	Tire Deflection (m)
19:24:34	0.03	**19:24:58**	-0.11	**19:25:22**	0.21
19:24:35	0.03	**19:24:59**	-0.14	**19:25:23**	0.14
19:24:36	0.07	**19:25:00**	0.06	**19:25:24**	0.12
19:24:37	0	**19:25:01**	0.14	**19:25:25**	0.03
19:24:38	-0.07	**19:25:02**	0.35	**19:25:26**	0.02
19:24:39	0.03	**19:25:03**	0.36	**19:25:27**	0.02
19:24:40	0.05	**19:25:04**	0.34	**19:25:28**	0.06
19:24:41	0.06	**19:25:05**	0.29	**19:25:29**	0.14
19:24:42	0.05	**19:25:06**	0.17	**19:25:30**	0.15
19:24:43	0.48	**19:25:07**	0.11	**19:25:31**	0.11
19:24:44	0.62	**19:25:08**	-0.09	**19:25:32**	0.1
19:24:45	0.6	**19:25:09**	-0.07	**19:25:33**	0.06
19:24:46	0.49	**19:25:10**	-0.02	**19:25:34**	0.04
19:24:47	0.03	**19:25:11**	0	**19:25:35**	0.04
19:24:48	-0.06	**19:25:12**	0.31	**19:25:36**	0.04
19:24:49	-0.14	**19:25:13**	0.31	**19:25:37**	0.04
19:24:50	-0.15	**19:25:14**	0.21	**19:25:38**	0.11
19:24:51	0.26	**19:25:15**	0.18	**19:25:39**	0.11
19:24:52	0.4	**19:25:16**	-0.01	**19:25:40**	0.1
19:24:53	0.48	**19:25:17**	-0.02	**19:25:41**	0.08
19:24:54	0.41	**19:25:18**	-0.02	**19:25:42**	0.08
19:24:55	0.39	**19:25:19**	-0.03	**19:25:43**	0.07
19:24:56	0.2	**19:25:20**	0.19	**19:25:44**	0.06
19:24:57	0	**19:25:21**	0.2	**19:25:22**	0.21

Table A-4: Experimental results for active, tire deflection

Time(ms)	Tire Deflection (m)	Time(ms)	Tire Deflection (m)	Time(ms)	Tire Deflection (m)
19:35:43	0.01	19:36:07	-0.08	19:36:31	0.01
19:35:44	0	19:36:08	-0.09	19:36:32	0.01
19:35:45	0.01	19:36:09	-0.02	19:36:33	0
19:35:46	0.11	19:36:10	0.01	19:36:34	0
19:35:47	0.07	19:36:11	0.16	19:36:35	0.02
19:35:48	-0.02	19:36:12	0.21	19:36:36	0.02
19:35:49	0.39	19:36:13	0.07	19:36:37	0.04
19:35:50	0.57	19:36:14	0.05	19:36:38	0.04
19:35:51	0.61	19:36:15	0.01	19:36:39	0.03
19:35:52	0.48	19:36:16	0	19:36:40	0.01
19:35:53	-0.04	19:36:17	-0.05	19:36:41	0.01
19:35:54	0.1	19:36:18	-0.03	19:36:42	0
19:35:55	-0.03	19:36:19	0.12	19:36:43	0.01
19:35:56	-0.08	19:36:20	0.11	19:36:44	0.02
19:35:57	-0.14	19:36:21	0.12	19:36:45	0.01
19:35:58	-0.1	19:36:22	0.11	19:36:46	0.03
19:35:59	0.02	19:36:23	0	19:36:47	0.02
19:36:00	0.44	19:36:24	-0.02	19:36:48	0.01
19:36:01	0.5	19:36:25	-0.01	19:36:49	0.01
19:36:02	0.28	19:36:26	0	19:36:50	0
19:36:03	0.32	19:36:27	0.02	19:36:51	0.01
19:36:04	0.12	19:36:28	0.07	19:36:52	0.01
19:36:05	0.07	19:36:29	0.08	19:36:53	0.02
19:36:06	-0.09	19:36:30	0.07		

Table A-5: Experimental results for passive, suspension travel

Time(ms)	Suspension Travel	Time(ms)	Suspension Travel	Time(ms)	Suspension Travel
21:29:22	0.21	21:29:46	0.14	21:30:10	0.24
21:29:23	0.19	21:29:47	0.19	21:30:11	0.21
21:29:24	0.24	21:29:48	0.00	21:30:12	0.28
21:29:25	0.15	21:29:49	-0.20	21:30:13	0.30
21:29:26	0.22	21:29:50	**-0.24**	21:30:14	0.26
21:29:27	0.21	21:29:51	-0.22	21:30:15	0.24
21:29:28	0.15	21:29:52	-0.16	21:30:16	0.22
21:29:29	0.18	21:29:53	0.04	21:30:17	0.31
21:29:30	0.22	21:29:54	0.12	21:30:18	0.29
21:29:31	0.19	21:29:55	0.31	21:30:19	0.30
21:29:32	0.21	21:29:56	**0.43**	21:30:20	0.28
21:29:33	0.26	21:29:57	0.26	21:30:21	0.21
21:29:34	0.20	21:29:58	0.18	21:30:22	0.22
21:29:35	0.15	21:29:59	0.11	21:30:23	0.19
21:29:36	0.22	21:30:00	-0.00	21:30:24	0.22
21:29:37	0.17	21:30:01	-0.12	21:30:25	0.20
21:29:38	0.14	21:30:02	-0.18	21:30:26	0.18
21:29:39	0.26	21:30:03	-0.16	21:30:27	0.22
21:29:40	0.19	21:30:04	-0.9	21:30:28	0.20
21:29:41	0.21	21:30:05	-0.02	21:30:29	0.28
21:29:42	0.22	21:30:06	0.01	21:30:30	0.23
21:29:43	0.16	21:30:07	-0.03	21:30:31	0.13
21:29:44	0.20	21:30:08	0.19	21:30:32	0.21
21:29:45	0.16	21:30:09	0.31		

Table A-6: Experimental results for active, suspension travel

Time(ms)	Suspension Travel	Time(ms)	Suspension Travel	Time(ms)	Suspension Travel
21:32:32	0.16	**21:32:56**	0.21	**21:33:20**	0.24
21:32:33	0.22	**21:32:57**	0.21	**21:33:21**	0.22
21:32:34	0.18	**21:32:58**	0.18	**21:33:22**	0.26
21:32:35	0.25	**21:32:59**	0.22	**21:33:23**	0.34
21:32:36	0.16	**21:33:00**	0.17	**21:33:24**	0.21
21:32:37	0.21	**21:33:01**	0.15	**21:33:25**	0.23
21:32:38	0.19	**21:33:02**	0.06	**21:33:26**	0.25
21:32:39	0.21	**21:33:03**	0.04	**21:33:27**	0.31
21:32:40	0.24	**21:33:04**	0.12	**21:33:28**	0.33
21:32:41	0.15	**21:33:05**	0.11	**21:33:29**	0.37
21:32:42	0.22	**21:33:06**	0.12	**21:33:30**	0.29
21:32:43	0.17	**21:33:07**	0.06	**21:33:31**	0.14
21:32:44	0.25	**21:33:08**	0.18	**21:33:32**	0.21
21:32:45	0.23	**21:33:09**	0.11	**21:33:33**	0.17
21:32:46	0.16	**21:33:10**	-0.06	**21:33:34**	0.16
21:32:47	0.19	**21:33:11**	-0.16	**21:33:35**	0.24
21:32:48	0.17	**21:33:12**	-0.22	**21:33:36**	0.19
21:32:49	0.15	**21:33:13**	-0.17	**21:33:37**	0.32
21:32:50	0.24	**21:33:14**	0.34	**21:33:38**	0.3
21:32:51	0.19	**21:33:15**	0.32	**21:33:39**	0.29
21:32:52	0.23	**21:33:16**	0.4	**21:33:40**	0.23
21:32:53	0.16	**21:33:17**	0.33	**21:33:41**	0.17
21:32:54	0.23	**21:33:18**	0.33	**21:33:42**	0.26
21:32:55	0.17	**21:33:19**	0.25		

Appendix B: Datasheets of sensors and actuators used in experimental model

Datasheet B-1: Flex Sensor

spectrasymbol

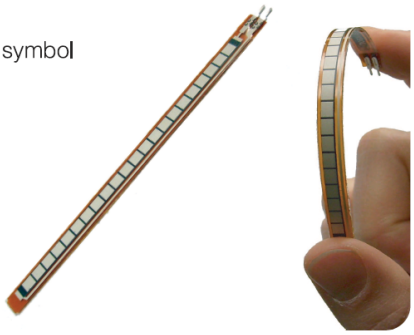

FLEX SENSOR FS

Features

- Angle Displacement Measurement
- Bends and Flexes physically with motion device
- Possible Uses
  - Robotics
  - Gaming (Virtual Motion)
  - Medical Devices
  - Computer Peripherals
  - Musical Instruments
  - Physical Therapy
- Simple Construction
- Low Profile

Mechanical Specifications

-Life Cycle: >1 million
-Height: ≤0.43mm (0.017")
-Temperature Range: -35°C to +80°C

Electrical Specifications

-Flat Resistance: 10K Ohms
-Resistance Tolerance: ±30%
-Bend Resistance Range: 60K to 110K Ohms
-Power Rating : 0.50 Watts continuous. 1 Watt Peak

Dimensional Diagram - Stock Flex Sensor

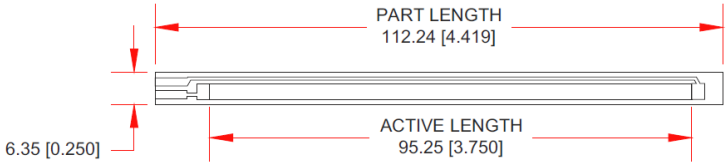

How to Order - Stock Flex Sensor

FS	–	L	–	0095	–	103	–	ST
Series		Model		Active Length		Resistance		Connectors
FS = Flex Sensor		L = Linear		0095 = 95.25mm		103 = 10 KOhms		ST = Solder Tab

How It Works

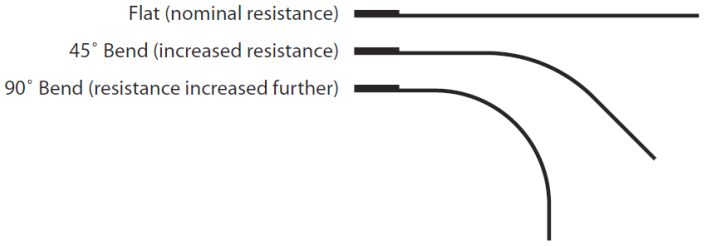

Datasheet B-1: Flex Sensor (Continued)

Schematics

BASIC FLEX SENSOR CIRCUIT:

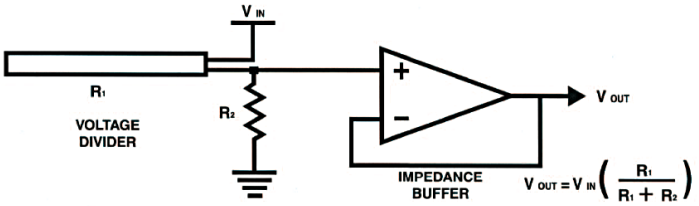

Following are notes from the ITP Flex Sensor Workshop

"The impedance buffer in the [Basic Flex Sensor Circuit] (above) is a single sided operational amplifier, used with these sensors because the low bias current of the op amp reduces errer due to source impedance of the flex sensor as voltage divider. Suggested op amps are the LM358 or LM324."

"You can also test your flex sensor using the simplest circut, and skip the op amp."

"Adjustable Buffer - a potentiometer can be added to the circuit to adjust the sensitivity range."

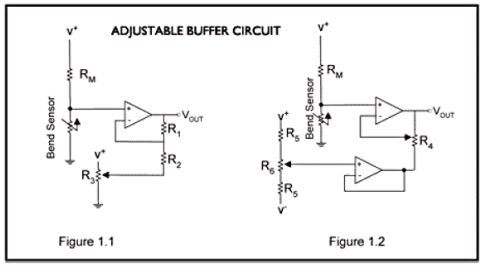

"Variable Deflection Threshold Switch - an op amp is used and outputs either high or low depending on the voltage of the inverting input. In this way you can use the flex sensor as a switch without going through a microcontroller."

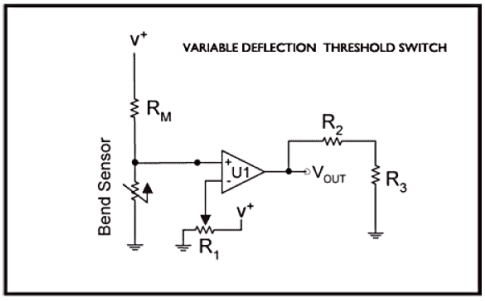

"Resistance to Voltage Converter - use the sensor as the input of a resistance to voltage converter using a dual sided supply op-amp. A negative reference voltage will give a positive output. Should be used in situations when you want output at a low degree of bending."

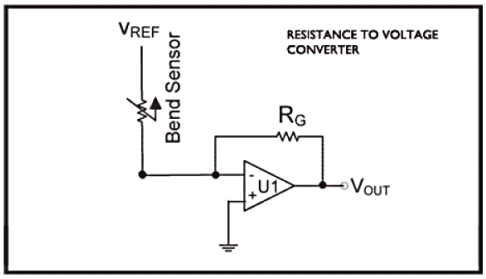

http://www.sparkfun.com/datasheets/Sensors/Flex/FLEXSENSOR (REVA1).pdf

Datasheet B-2: Example of datasheet helps for stiffness calculation in air-spring.

	Description	Assembly Order No.
Style 7012 Two Ply Bellows	Blind nut, 1/8 NPT	W02-358-7002
Assembly weight ..... .82 kg.		

NOTE: Standard assembly is imperial.

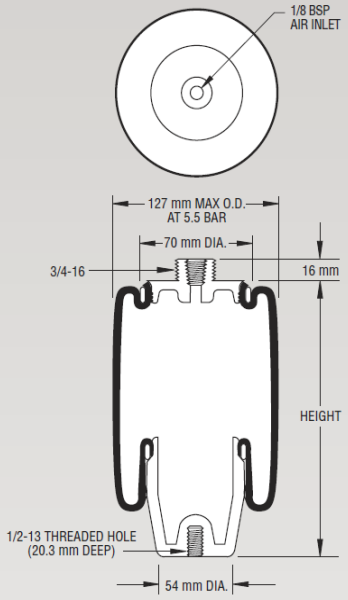

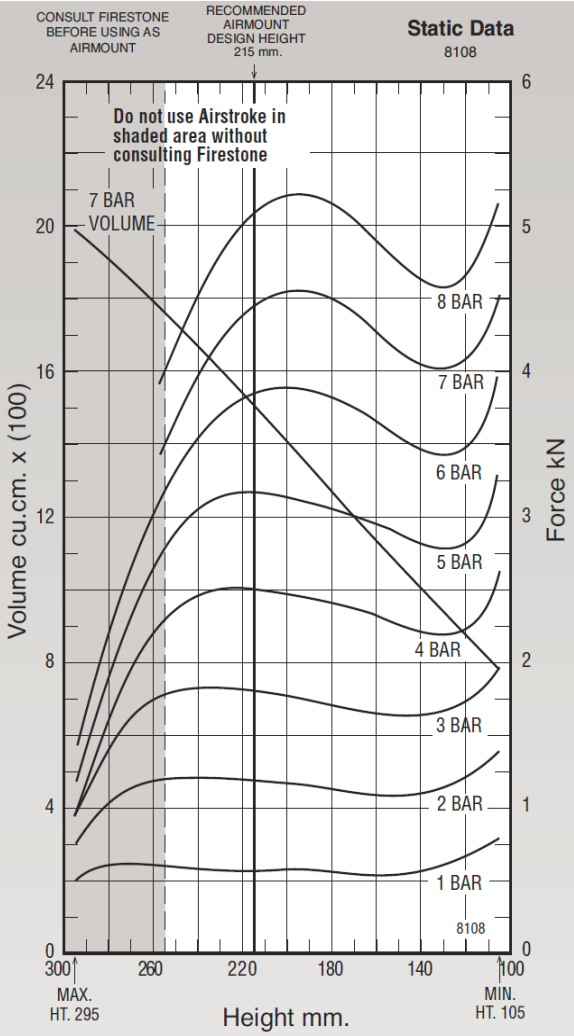

See page 12 for instructions on how to use chart.

NOTE: Bellows will not compress properly with less than .7 BAR internal pressure.

Dynamic Characteristics at 215 mm Design Height
(Required for Airmount isolator design only)

Gauge Pressure (BAR)	Load (kN)	Spring Rate (kN/m)	Natural Frequency Hz
3	1.81	13	1.31
4	2.51	18	1.33
5	3.18	23	1.33
6	3.85	33	1.47
7	4.44	43	1.55

Force Table (Use for Airstroke™ actuator design)

Assembly Height (mm)	Volume @ 7 BAR (cu cm)	EFF Area @ 7 BAR (cm sq)	kN Force @ 3 BAR	@ 4 BAR	@ 5 BAR	@6 BAR	@7 BAR
240	1676	56	1.83	2.45	3.06	3.52	3.94
220	1547	62	1.82	2.52	3.18	3.81	4.37
200	1409	65	1.77	2.48	3.15	3.89	4.56
180	1271	65	1.71	2.42	3.07	3.83	4.51
160	1134	61	1.65	2.33	2.97	3.67	4.30
140	1000	58	1.63	2.22	2.83	3.48	4.06

Datasheet B-3: Solid Relay.

OPTO 22

I/O MODULE
G4 DIGITAL
DC OUTPUT

DATA SHEET

Form 254-990215

Part Number	Description
G4ODC5	G4 DC Output 5-60 VDC, 5 VDC Logic
G4ODC5A	G4 DC Output 5-200 VDC, 5 VDC Logic
G4ODC5MA	G4 DC Output 5-60 VDC, 5 VDC Logic With Manual/Auto Switch
G4ODC15	G4 DC Output 5-60 VDC, 15 VDC Logic
G4ODC24	G4 DC Output 5-60 VDC, 24 VDC Logic
G4ODC24A	G4 DC Output 5-200 VDC, 24 VDC Logic

Description

Opto 22's G4 DC output modules are used to control or switch DC loads. Each module provides up to 4,000 V_{rms} of optical-isolation between field devices and control logic.

The G4ODC5MA is a special module featuring a manual-on/manual-off/automatic switch, ideal for diagnostic testing of control applications.

Typical applications for DC output modules include switching loads such as DC relays, solenoids, motor starters, lamps, and indicators.

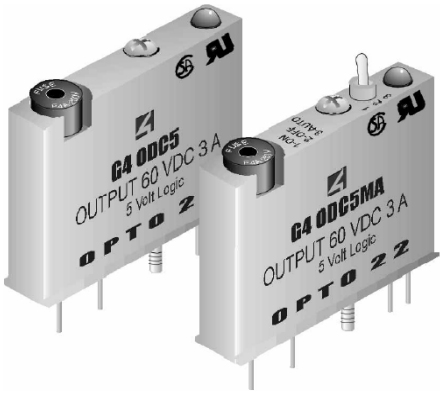

Features

- 4,000 V_{rms} optical-isolation
- Built-in LED status indicator
- Logic levels of 5, 15, and 24 VDC
- Removable fuse
- Ability to withstand one-second surge of 5 amps
- Operating temperature: -30° C to 70° C
- UL recognized, CSA certified, CE approved
- Passes NEMA Showering Arc Test (ICS 2-230)
- Meets IEEE Surge Withstand Specification (IEEE-472)

	Units	G4ODC5*	G4ODC5A*	G4ODC5MA*	G4ODC15	G4ODC24	G4ODC24A
Maximum line voltage	VDC	60	200	60	60	60	200
Output voltage range	VDC	5-60	5-200	5-60	5-60	5-60	5-200
Key feature		---	---	Diagnostic switch	---	---	---
Current rating: at 45°C ambient at 70°C ambient	A A	3 2	1 0.55	3 2	3 2	3 2	1 0.55
Isolation input-to-output	V_{rms}	4,000	4,000	4,000	4,000	4,000	4,000
Off-state leakage at maximum voltage	mA	1	2	1	1	1	2
Control resistance (R_C in schematic)	Ω	220	220	220	1K	2.2K	2.2K
One-second surge	A	5	5	5	5	5	5
Turn-on time	µs	50	100	50	50	50	100
Turn-off time	µs	50	750	50	50	50	750
Output voltage drop maximum peak	V	1.6	1.6	1.6	1.6	1.6	1.6
Nominal logic voltage	VDC	5	5	5	15	24	24
Logic voltage range	VDC	4-8	4-8	4-8	10.5-16	19.5–32	19.5–32
Logic pickup voltage	VDC	4	4	4	10.5	19.5	19.5
Logic dropout voltage	VDC	1	1	1	1	1	1
Logic input current at nominal logic voltage	mA	12	12	12	15	18	18
Temperature: Operating Storage	°C °C	-30 to +70 -30 to +85	-30 to +70 -30 to +85	-30 to +70 -30 to +85	-30 to +70 -30 to +85	-30 to +70 -30 to +85	-30 to +70 -30 to +85

Datasheet B-3: Solid Relay. (Continued)

Dimensions

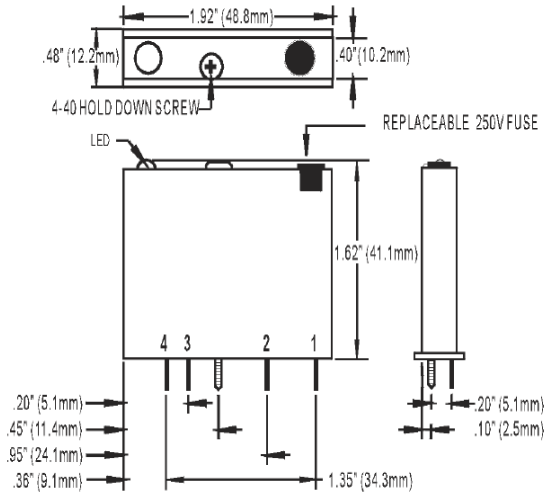

Schematics

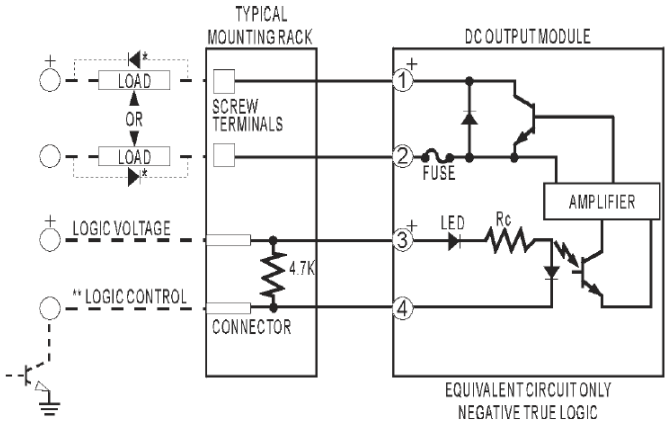

* Commutation diode must be used on inductive loads. Typically, use diode IN4005.
** Control line is compatible with totem pole or tri-state output device.

Datasheet B-4: Solenoid Valve.

Solenoid valves are an efficient method of converting electrical signals into pneumatic functions. Applying electricity to the solenoid quickly directs air through the valve and into the circuit.
Valves can be designated as internally piloted or externally piloted. Externally piloted valves use an external source of air pressure. Internally piloted use an internal source of air pressure.
Solenoid valves are controlled by the action of the solenoid and typically control the flow of water or air as a switch. If the solenoid is active (current is applied), it opens the valve. If the solenoid is inactive (current does not exist), the valve stays closed.

Product name: **4V230C-08 Solenoid Valve**
Model Number: SL-4V230C-08

---- 4V230C-08 Solenoid Valve

Specification of **4V230C-08 Series Solenoid Valve**:

Model	4V210-08	4V220-08	4V230C-08	4V230E-08	4V230P-08
Operation Type	Inside Pilot Type				
Fluid Medium	40 Micron Filtered Air				
Position and Way Number	Two-Position Five Way		Three-Position Five Way		
Working Pressure	0.15--0.8Mpa(21--114psi)				
Proof Pressure	1.2MPa(174psi)				
Working Temperature	5--50℃				
Port Size	Air Inlet=Air Outlet=G1/4, Exhaust=G1/8				
Material	Aluminium Alloy				
Highest Action Frequency	5 Cycles/second				
Effective Sectional Area	16mm2(Cv=0.89)		12mm2(Cv=0.67)		
Shortest Excitation Time	0.05 Second				
Weight	220g	320g	400g		

4V230c-08, with same port size of **4V210-08** and **4V220-08 Solenoid valve**, is however, three position, five way type solenoid valve.
4V230C-08 solenoid valves have applications in medical industry like Oxygen Concentrators, Blood Pressure Testing Equipment, CPR Devices, Angioplasty Devices, Anesthesiology Delivery Systems, Optical Grinding Equipment.
Ordering Code of **4V230 Series Solenoid Valve**:

Ordering code

4V	2	230	-	08
Specification	**Series**	**Coil and places**		**Port size**
4V:5/2(3) way solenoid valve 4A:5/2(3) way pneumatic control valve 3V:3/2 way solenoid valve 3A:3/2 way pneumatic control valve	200 series	10:Single-head double-position 20:Double-head double-position 30C:Double-head three-position close centre 30E:Double-head three-position exhaust centre 30P:Double-head three-position Pressure centre		06: 1/8″ 08: 1/4″

www.chinapropneumatic.com

http://pneumatic-components.en.hisupplier.com/product-811356-4V230C-08-Solenoid-Valve.html

Datasheet B-5: Data Acquisition Card.

ECONseries

Low Cost USB Data Acquisition Modules

ECONseries

Low Cost USB DAQ

The ECONseries is a flexible yet economical series of multifunction data acquisition modules. You choose the number of analog I/O and digital I/O channels, the resolution you need, and the signal range of your application.

Key Features:

- **Ultimate flexibility** with up to 24 analog inputs, 2 analog outputs, 28 digital I/O, and one 32-bit counter timer
- **10-, 12-, or 16-bit resolution**
- **Independent subsystem operation** at throughput rates up to 750 kHz per channel
- **Simultaneous analog inputs** on the DT9816 modules
- **Signal range of ±10V** on both the analog input and analog output, DT9812-2.5V has analog signal range of 0-2.44V
- **Generate sine, rectangle, triangle, or DC waveforms** with the analog outputs
- **Three versions of Digital I/O** modules: isolated, non-isolated, and high current drive
- **Monitor and control** up to 28 digital I/O lines
- **Perform event counting,** frequency measurement, edge-to-edge measurement, and rate generation (continuous pulse output) operations using 32-bit counter/timer
- **Shielded, rugged enclosure** for noise immunity, with built-in screw terminals

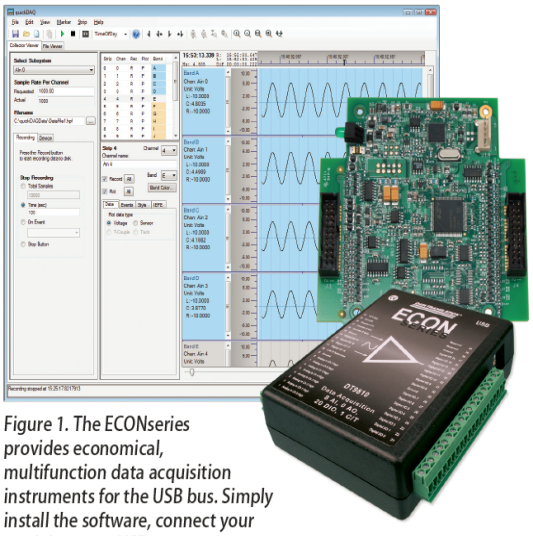

Figure 1. The ECONseries provides economical, multifunction data acquisition instruments for the USB bus. Simply install the software, connect your module to any USB port, and measure.

- **Easy signal connections on the DT9812-10V-OEM and the DT9816-OEM** with two 20-pin connectors for all I/O signals
- **All modules** run off USB power supply, no external power supply needed

Features Summary								
Module	Analog Inputs	Resolution	I/O Range	Analog Input Sample Rate	Analog Outputs	Analog Output Update Rate	Digital I/O	C/T
DT9810	8 SE	10-bit	0 to 2.44V	25 kS/s aggregate	—	—	20 I/O	1
DT9812-2.5V	8 SE	12-bit	0 to 2.44V, 1.22V, 0.61V, 0.305V, 0.1525V	50 kS/s aggregate	2	50 kS/s	8 in/8 out	1
DT9812-10V DT9812-10V-OEM	8 SE	12-bit	±10V, ±5V, ±2.5V, ±1.25V	50 kS/s aggregate	2	50 kS/s	8 in/8 out	1
DT9812A	8 SE	12-bit	±10V, ±5V, ±2.5V, ±1.25V	100 kS/s aggregate	2	75 kS/s	8 in/8 out	1
DT9813-10V	16 SE	12-bit	±10V, ±5V, ±2.5V, ±1.25V	50 kS/s aggregate	2	50 kS/s	4 in/4 out	1
DT9813A	16 SE	12-bit	±10V, ±5V, ±2.5V, ±1.25V	100 kS/s aggregate	2	75 kS/s	4 in/4 out	1
DT9814-10V	24 SE	12-bit	±10V, ±5V, ±2.5V, ±1.25V	50 kS/s aggregate	2	50 kS/s	—	1
DT9814A	24 SE	12-bit	±10V, ±5V, ±2.5V, ±1.25V	100 kS/s aggregate	2	75 kS/s	—	1
DT9816 DT9816-OEM	6 SE	16-bit	±10V or ±5V	50 kS/s per ch	—	—	8 in/8 out	1
DT9816-A	6 SE	16-bit	±10V or ±5V	150 kS/s per ch	—	—	8 in/8 out	1
DT9816-S	6 SE	16-bit	±10V or ±5V	750 kS/s per ch	—	—	8 in/8 out	1
DT9817	—	—	—	—	—	—	28 I/O	1
DT9817-H	—	—	—	—	—	—	28 I/O High Drive	1
DT9817-R	—	—	—	—	—	—	8 in/8 out Isolated High Drive	1

Datasheet B-5: Data Acquisition Card. (Continued)

DT9812 Block Diagram

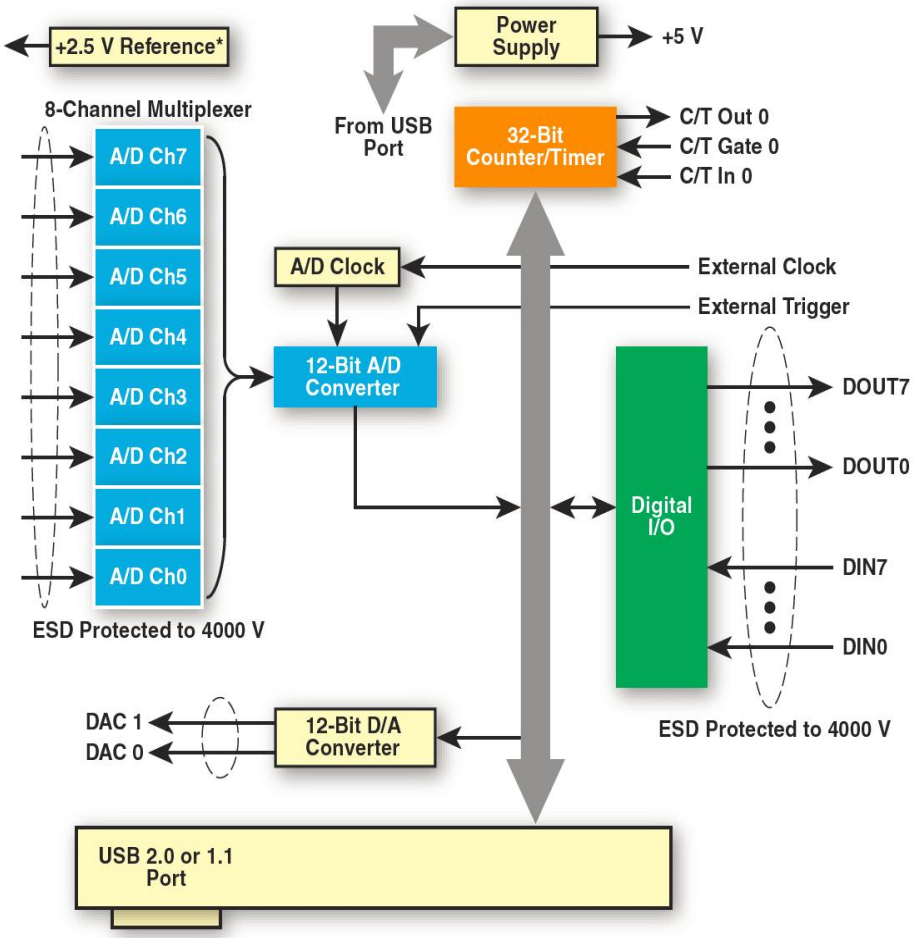

Figure 2. Block Diagram of the DT9812-2.5V, DT9812-10V, DT9812-10V-OEM, and DT9812A Modules.

DT9812-10V DT9812-10V-OEM

Figure 3. All DT9812 versions provide 8 analog inputs with 12-bit resolution, 2 analog outputs, 16 digital I/O, and 1 C/T.

Datasheet B-6: Pressure Sensor.

Cole-Parmer® High-Accuracy Industrial Pressure Transducers

Withstands high shock and vibration applications

- Welded stainless steel (SS) housing rated to NEMA 4 (IP65) standards

Transducers feature SS capacitive sensor for your more demanding systems—even ElectroMagnetic Interference (EMI)/Radio Frequency Interference (RFI) resistance ensures accurate and consistent performance in any environment.

Transducers feature adjustable zero and span potentiometers. Transducers with 4 to 20 mA output have red (positive power) and black (output) wires. Transducers with 0.1 to 5.1 V output have red (positive power), green (output), and white/black (common) wires.

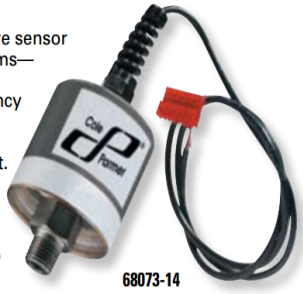

68073-14

Specifications

ISO 9001:2000 CERTIFIED SUPPLIER

Accuracy: ±0.13% full-scale
Operating temperature: –40 to 260°F (–40 to 126°C)
Process connection: 1/4" NPT(M)
Power: 12 to 28 VDC (unregulated)
Electrical connection: 2-ft L cable
Wetted materials: 17-4PH stainless steel
Dimensions: 5"L x 2" diameter

Range	4 to 20 mA output		0.1 to 5.1 V output	
	Catalog number	Price	Catalog number	Price
Compound transducers				
–14.7 to 15 psi	RZ-68073-00		RZ-68074-00	
–14.7 to 30 psi	RZ-68073-02		RZ-68074-02	
–14.7 to 60 psi	RZ-68073-04		RZ-68074-04	
–14.7 to 100 psi	RZ-68073-06		RZ-68074-06	
Gauge pressure transducers				
0 to 25 psig	RZ-68073-08		RZ-68074-08	
0 to 50 psig	RZ-68073-10		RZ-68074-10	
0 to 100 psig	RZ-68073-12		RZ-68074-12	
0 to 500 psig	RZ-68073-14		RZ-68074-14	
0 to 1000 psig	RZ-68073-16		RZ-68074-16	
0 to 3000 psig	RZ-68073-18		RZ-68074-18	
0 to 5000 psig	RZ-68073-20		RZ-68074-20	
0 to 10,000 psig	RZ-68073-22		RZ-68074-22	

RZ-17040-12 **NIST-traceable calibration certificate** .....